REALIZATION OF TRANSFER IMPEDANCES

USING DISTRIBUTED RC ELEMENTS

IN

A COMMON GROUND LINVILL CONFIGURATION

BY

WALTER WORONKA

A THESIS

PRESENTED IN PARTIAL FULFILLMENT OF

THE REQUIREMENTS FOR THE DEGREE

OF

MASTER OF SCIENCE IN ELECTRICAL ENGINEERING

AT

NEWARK COLLEGE OF ENGINEERING

Newark, New Jersey
1968

APPROVAL OF THESIS

REALIZATION OF TRANSFER IMPEDANCES

USING DISTRIBUTED RC ELEMENTS

IN

A COMMON GROUND LINVILL CONFIGURATION

BY

WALTER WORONKA

FOR

DEPARTMENT OF ELECTRICAL ENGINEERING

BY

FACULTY COMMITTEE

APPROVED: _____

_____

_____

NEWARK, NEW JERSEY

JUNE, 1968

ABSTRACT

One of several synthesis procedures available for the realization of a transfer admittance is that of Linvill. This synthesis procedure employs an active element, a negative impedance converter (NIC), to shift the poles of passive immittance functions from the negative real axis into the complex plane to realize the desired transfer immittance function.

The Linvill synthesis procedure is extended to networks containing cascaded distributed RC elements and the conditions which must be satisfied to realize a transfer impedance using these distributed elements are defined.

ACKNOWLEDGEMENT

TABLE OF CONTENTS

CHAPTER I. INTRODUCTION TO ACTIVE FILTERS

1-1 Area of Investigation

Active $\overline{RC}$ filters have become practical, reliable and precise due to the advancing technology of monolithic and thin film integrated circuit development and fabrication. The application of microminiatureization techniques has resulted in lower cost; improvement of system reliability and significant reduction of size. The practicality of active networks is a direct result of the availability of stable resistors and capacitors of small size with compensated temperature coefficients.

Since active elements have become compatible with passive networks, several active network realization procedures for driving point and transfer immittances, and transfer voltage ratios have resulted.[1-6] The active element employed may be either a negative impedance converter,[7] a high gain stabilized feedback amplifier or a gyrator. The active elemement simply is used to shift the poles of passive immittance functions from the negative real axis into the complex plane to realize the desired immittance function. The ability to control the pole and zero locations in the S-plane using an active element permits the design of highly selective

low pass, high pass as well as band pass networks
without the use of inductors.

This paper defines the conditions which must
be satisfied to realize a transfer impedance via the
Linvill network configuration, using cascaded $\overline{RC}$
elements. The specific configuration is shown in
Figure 13.

1-2   Historic Background

A uniform distributed RC element[8,9] is defined
as a distributed transmission line having only series
resistance and shunt capacitance uniformly distributed
per unit length. The distributed $\overline{RC}$ structure is of
multi-layer construction with the resistive layer and
the capacitive layer separated by a dielectric as shown
in Figure 1. In general the $\overline{RC}$ element is constructed
such that the length is much greater than the width. The
inductance of a typical element is negligible below
100 KHz.

In 1963, significant progress in the area of
exact network synthesis of distributed RC networks was
made by Wyndrum[8]. The synthesis procedure utilizes a
positive real mapping technique which transforms the
transcendental expressions characterized by a distribu-
ted element into the simpler, non-transcendental form
or finite polynomials. This transformation results in
lumped LC functions growing out of the original RC
functions, permitting the use of network theory[10-13]
developed specifically for lumped LC functions. Wyndrum
shows that the repeated use of Richard's theorem[14] to
extract unit RC sections from a desired impedance
function results in the realization of the desired
transfer or driving point function by a cascade
of a finite number of RC sections.

A method for the realization of transmission zeros was presented using a stub as a zero preparation element followed by extraction of other RC elements to complete the realization of the desired transmission zeros.

In 1965, O'Shea[9] presented a synthesis procedure for driving point and transfer functions using an equivalent transformation technique. The synthesis procedure for the driving point impedance was identical in capabilities to that presented by Wyndrum, but did not necessarily result in a common ground network.

Work in the area of passive distributed network synthesis progressed with the cascade synthesis of distributed networks presented by Scanlan and Rhodes[15]. Their development used the transformation presented by Wyndrum and is restricted to functions which may be realized by a cascade of two-port RC sections, series or short-circuited stubs, and shunt open-circuited stubs leading to rational functions after transformation. Another restriction imposed was that the network elements all had commensurate lenth, i.e. $RC = \sqrt{\tau}$ or multiples thereof for each section. Necessary conditions for realization of any short circuit or open circuit immittance parameters together with the sufficiency condition for simultaneous realization of any two such

parameters have been formulated.

In 1966, Stein, Mulligan, and Shamis [16] developed
the necessary and sufficient conditions for the realiza-
tion of open-circuit $\overline{URC}$ voltage transfer functions. The
synthesis is in the form of commensurate length having
a common ground connection. The cascade network is
composed of realization cycles containing a "zero
preparation" element followed by an RC element and
finally followed by a series or shunt stub to realize
the transmission zero. An extraction technique using
Richard's theorem was used to realize the transmission
zeros of the desired function. The authors used the
transformation presented by Wyndrum with an additional
step of transforming from the lumped LC plane to the
lumped RC plane.

CONDUCTIVE LAYER
DIELECTRIC LAYER
RESISTIVE LAYER
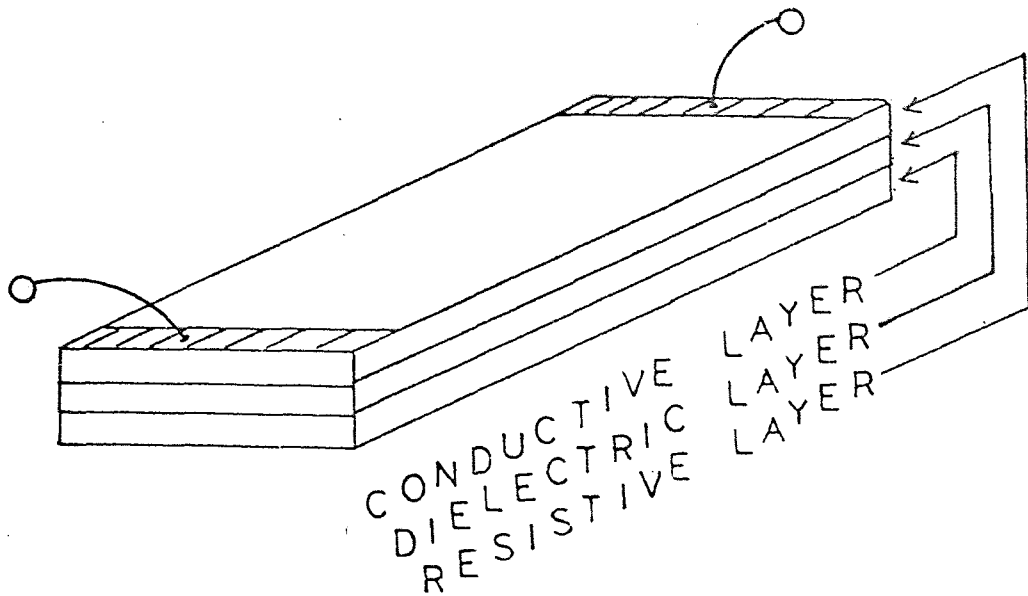
PHYSICAL STRUCTURE
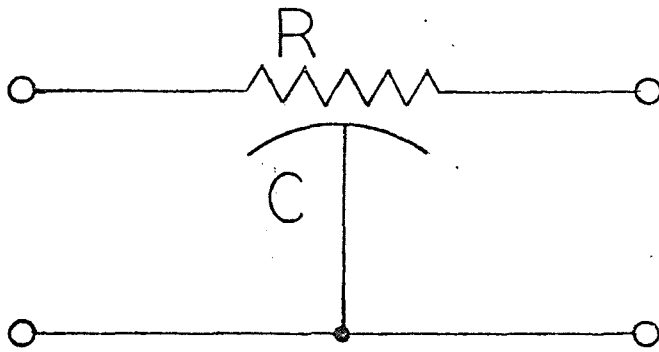
SYMBOLIC REPRESENTATION

FIGURE 1

CHAPTER II. MATHEMATICAL CHARACTERIZATION OF ACTIVE

RC NETWORKS

2-1 Properties of URC Elements

2-1.1 Basic Characteristics. A uniform $\overline{RC}$ line open cir-

cuited segment, shown in Figure 2, is characterized

by the ABCD parameters[8] .

$$\begin{vmatrix} A & B \\ C & D \end{vmatrix} = \begin{vmatrix} \cosh\sqrt{RCS} & \dfrac{R\sinh\sqrt{RCS}}{\sqrt{RCS}} \\ \dfrac{\sqrt{RCS}\,\sinh\sqrt{RCS}}{R} & \cosh\sqrt{RCS} \end{vmatrix} \qquad (2\text{-}1)$$

where R and C are in ohms per unit length and

farads per unit length respectively. The equivalent

Z-parameters for the single $\overline{RC}$ segment are

$$\begin{vmatrix} Z_{11} & Z_{12} \\ Z_{21} & Z_{22} \end{vmatrix} = \begin{vmatrix} \dfrac{R\coth\sqrt{RCS}}{\sqrt{RCS}} & \dfrac{R\operatorname{csch}\sqrt{RCS}}{\sqrt{RCS}} \\ \dfrac{R\operatorname{csch}\sqrt{RCS}}{\sqrt{RCS}} & \dfrac{R\coth\sqrt{RCS}}{\sqrt{RCS}} \end{vmatrix} \qquad (2\text{-}2)$$

The expression for the transfer impedance for a

single open-circuited $\overline{RC}$ element is given by

$$Z_{21}(S) = \frac{R\operatorname{csch}\sqrt{RCS}}{\sqrt{RCS}} \qquad (2\text{-}3)$$

and is characterized by a pole at the origin

followed by an infinite number of discrete poles

in the S-plane positioned on the negative real axis.
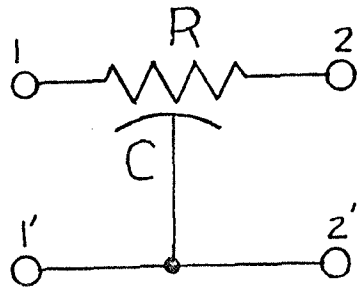
$$Z_{11} = \frac{R\,\mathrm{coth}\,\sqrt{RCS}}{\sqrt{RCS}} \implies \frac{R\,\mathrm{coth}\,\sqrt{RCS}}{\sqrt{RC}} \implies \frac{\propto}{W}$$

$$Z_{21} = \frac{R\,\mathrm{csch}\,\sqrt{RCS}}{\sqrt{RCS}} \implies \frac{R\,\mathrm{csch}\,\sqrt{RCS}}{\sqrt{RC}} \implies \frac{\propto}{W\left(1-W^2\right)^{\frac{1}{2}}}$$

S-PLANE
($\overline{RC}$ PLANE)

$Z_{\overline{RC}}(S)$

$\sqrt{S}$ PLANE
($\overline{LC}$ PLANE)

$Z_{\overline{LC}}(\sqrt{S})$

W PLANE
(LC PLANE)

$Z_{LC}(W)$

FIGURE 2

6

The pole locations of Z_{21} are located at

$$S = -\frac{\pi^2 n^2}{\tau} \qquad (2\text{-}4)$$

where $\tau = RC$ and $n = 0, 1, 2, \ldots \infty$

A transmission zero is located at infinity.

Since a single open-circuited uniform $\overline{RC}$ element is both bilateral and symmetrical, the roots of Z_{12} and Z_{21} are identical. The open circuit driving point impedances are given by

$$Z_{11} = Z_{22} = \frac{R \coth\sqrt{\tau s}}{\sqrt{\tau s}} \qquad (2\text{-}5)$$

The poles of the driving point impedances are located at

$$S = -\frac{\pi^2 n^2}{\tau} \qquad n = 0, 1, 2, \ldots \infty \qquad (2\text{-}6)$$

and the zeros are located at

$$S = -\frac{(n + \frac{1}{2})^2 \pi^2}{\tau} \qquad n = 0, 1, 2, \ldots \infty \qquad (2\text{-}7)$$

in the S-plane respectively, as shown in Figure 3.

The poles of the driving point and transfer impedances are negative real in the S-plane. Consider the case when two $\overline{RC}$ elements of the same time constant are cascaded as shown in Figure 4. The ABCD parameters for this case are given by

$$\left|
\begin{array}{cc}
\cosh^2\sqrt{\tau s} + \frac{R_1}{R_2}\sinh^2\sqrt{\tau s} & \dfrac{(R_1 + R_2)\cosh\sqrt{\tau s}\,\sinh\sqrt{\tau s}}{\sqrt{\tau s}} \\[3mm]
\dfrac{R_1 R_2 \sqrt{\tau s}\,\cosh\sqrt{\tau s}\,\sinh\sqrt{\tau s}}{(R_1 + R_2)} & \cosh^2\sqrt{\tau s} + \frac{R_2}{R_1}\sinh^2\sqrt{\tau s}
\end{array}
\right| \qquad (2\text{-}8)$$
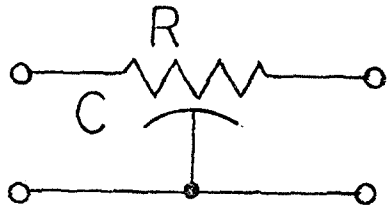
$$Z_{11}(S) = \frac{R \coth \sqrt{RCS}}{\sqrt{RCS}} \qquad Z_{21}(S) = \frac{R \operatorname{csch} \sqrt{RCS}}{\sqrt{RCS}}$$
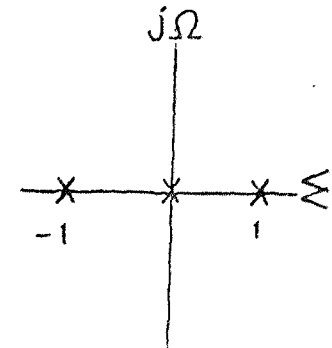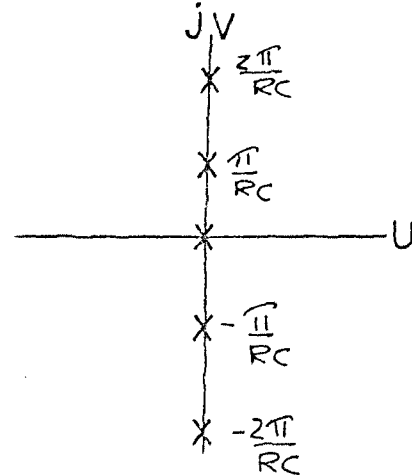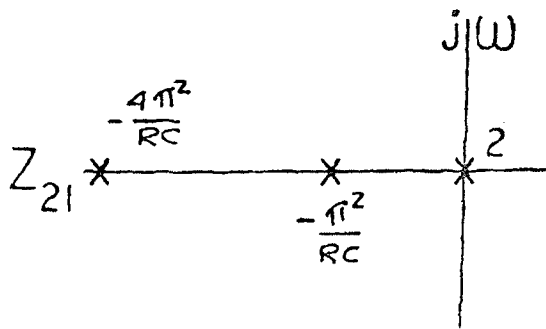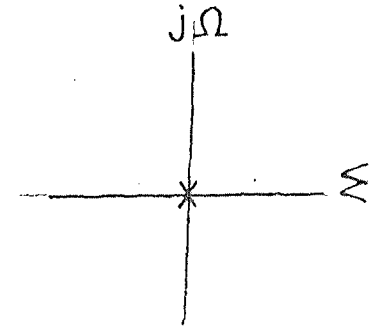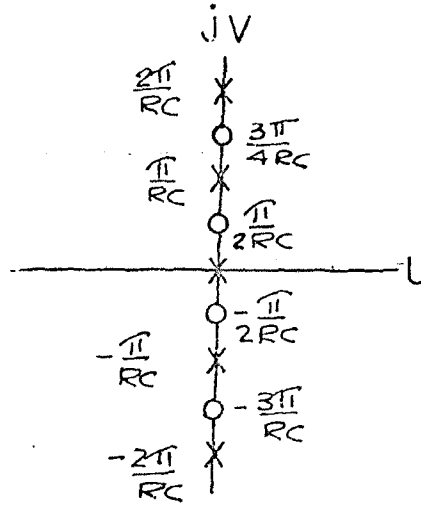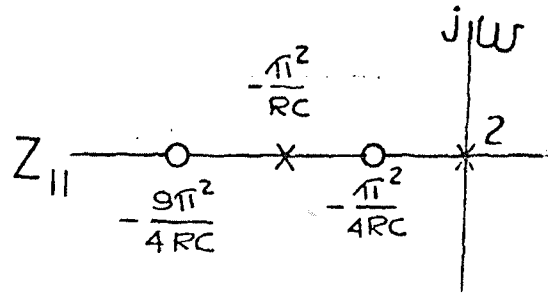
S-PLANE   S-PLANE   W-PLANE

FIGURE 3

The driving point impedance using (2-8) is given by

$$Z_{11} = \frac{(R_1 + R_2)\left[\cosh^2 \sqrt{\tau S} + \frac{R_1}{R_2} \sinh^2 \sqrt{\tau S}\right]}{R_1 R_2 \sqrt{\tau S} \cosh \sqrt{\tau S} \sinh \sqrt{\tau S}} \qquad (2\text{-}9)$$

The zeros of Z_{11} are the roots of

$$\tanh^2 \sqrt{\tau S} + \frac{R_2}{R_1} = 0 \qquad (2\text{-}10)$$

where (2-10) is equivalent to equation (8) in Appendix C. The solution given by (19) and (21) in Appendix C in terms of the constants under consideration here are given by

$$S_1 = -\frac{1}{4\tau}\left[2\pi r_1 - 2\tan^{-1}\sqrt{\frac{R_2}{R_1}}\right]^2_{r_1 = 0, 1, 2, \ldots} \qquad (2\text{-}11)$$

and

$$S_2 = -\frac{1}{4\tau}\left[\pi r_2 - 2\tan^{-1}\sqrt{\frac{R_2}{R_1}}\right]^2_{r_2 = 1, 2, \ldots} \qquad (2\text{-}12)$$

A transmission zero at infinity arises from the term $\frac{1}{\sqrt{\tau S}}$

The poles of Z_{11} are the roots of the equation

$$\sqrt{\tau S} \cosh \sqrt{\tau S} \sinh \sqrt{\tau S} = 0 \qquad (2\text{-}13)$$

The poles are located on the negative real axis in the S-plane at the locations given by

$$\left.\begin{array}{l} S = 0 \\ = -\dfrac{\pi^2 n^2}{\tau} \\ = -\dfrac{(n + \frac{1}{2})^2 \pi^2}{\tau} \end{array}\right\} \quad n = 0, 1, 2, \ldots \qquad (2\text{-}14)$$

The transfer impedance Z_{21_T} for an open circuited
two section $\overline{RC}$ element connected in cascade is
given by

$$Z_{21_T} = \frac{R_1 + R_2}{R_1 R_2 \sqrt{\tau s} \cosh\sqrt{\tau s} \sinh\sqrt{\tau s}} \qquad (2\text{-}15)$$

with subsequent pole locations in the S-plane
given by

$$\left. \begin{array}{l} S = - \dfrac{(n + \frac{1}{2})^2 \pi^2}{\tau} \\[2mm] = - \dfrac{\pi^2 n^2}{\tau} \end{array} \right\} \quad n = 0, 1, 2, \ldots \qquad (2\text{-}16)$$

Associated with (2-15) is also a transmission zero
at infinity.

In general, $\overline{RC}$ elements in cascade do not produce
any complex poles. All the singularities of the
driving point impedance and the transfer impedance
lie on the negative real axis in the S-plane.

2-1.2   <u>Transformation and Mapping</u>. Distributed elements,
being characterized by hyperbolic functions,
provide an infinite number of distinct poles and
zeros in the S-plane immittances. Due to the
large number of singularities in the immittance
functions, they become difficult to handle, in
order to conceptually visualize the frequency
response and shape of the functions under
consideration. Fortunately, it is possible to
conformally map these transcendental functions
into other complex planes where the original
functions themselves become simpler, being
represented by rational polynomials of a new
variable.

The first transformation[12] carries the
distributed $\overline{RC}$ plane expressions to the distri-
buted LC plane

$$Z_{\overline{LC}}(\sqrt{S}) = \sqrt{S}\ Z_{\overline{RC}}(S) \qquad (2\text{-}17)$$

Proceeding conversely, from the distributed LC
plane to the distributed $\overline{RC}$ plane

$$Z_{\overline{RC}}(S) = \frac{Z_{\overline{LC}}(\sqrt{S})}{\sqrt{S}} \qquad (2\text{-}18)$$

The transformation given by (2-17) still contains
infinitely many poles and/or zeros in the
immittance functions but these singularities are
shifted from the negative real axis in the

S-plane to the positive and negative imaginary axis in the $\sqrt{S}$ plane; they remain equally spaced. An additional transformation[8]

$$W = \tanh\sqrt{S}$$

is required to provide functions that may be realized in terms of finite polynomials. This transformation results in lumped LC functions in the W-plane which may be analyzed using network theory developed specifically for lumped elements. The S-plane to W-plane transformation of Z_{11} and Z_{21} parameters for two distributed RC elements in cascade is shown in Figure 4.

It is necessary to become familiar with the $S \to \sqrt{S} \to W$ transformation and the mechanics by which the infinite number of poles and zeros become finite terms in the W-plane. The relationship of the W-plane coordinates $W = \Sigma_1 + j\Omega_1$ in terms of the $\sqrt{S}$ plane coordinates are developed in Appendix A via equations (6) and (7) and are given below

$$\Sigma_1 = \frac{\sinh\sqrt{\tau}\,U \,\cosh\sqrt{\tau}\,U}{\cos^2\sqrt{\tau}\,V + \sinh^2\sqrt{\tau}\,U} \qquad (2\text{-}19)$$

$$\Omega_1 = \frac{\sin\sqrt{\tau}\,V \,\cos\sqrt{\tau}\,U}{\cos^2\sqrt{\tau}\,V + \sinh^2\sqrt{\tau}\,U} \qquad (2\text{-}20)$$

In Figure 5, various regions are identified in

$$R_1 C_1 = R_2 C_2$$

$$Z_{11} = \frac{1 + \frac{R_1}{R_2} \text{TANH}^2 (R_1, R_2)}{\sqrt{\tau s} \ \text{TANH} \sqrt{\tau s} \ (R_1 + R_2)}$$

$$Z_{11} = \frac{1 + \frac{R_1}{R_2} \text{TANH}^2 \sqrt{\tau s} (R_1, R_2)}{\sqrt{\tau} \ \text{TANH} \sqrt{\tau s} (R_1 + R_2)}$$

$$Z_{11} = \frac{1 + \frac{R_1}{R_2} W^2 (R_1, R_2)}{W \sqrt{\tau} (R_1 + R_2)}$$

$$Z_{21} = \frac{R_1 R_2}{\sqrt{\tau s} (R_1 + R_2) \text{COSH} \sqrt{\tau s} \ \text{SINH} \sqrt{\tau s}}$$

$$Z_{21} = \frac{R_1 R_2}{\sqrt{\tau} (R_1 + R_2) \text{COSH} \sqrt{\tau s} \ \text{SINH} \sqrt{\tau s}}$$

$$Z_{11} = \frac{(1 - W^2) R_1 R_2}{W \sqrt{\tau} (R_1 + R_2)}$$

S - PLANE
($\overline{RC}$ PLANE)

$Z_{\overline{RC}}(s)$

$\sqrt{S}$ - PLANE
($\overline{LC}$ PLANE)

$Z_{\overline{LC}} (\sqrt{S})$

W - PLANE
(LC PLANE)

$Z_{LC}(W)$

FIGURE 4

IDENTIFICATION OF CORRESPONDING
REGIONS
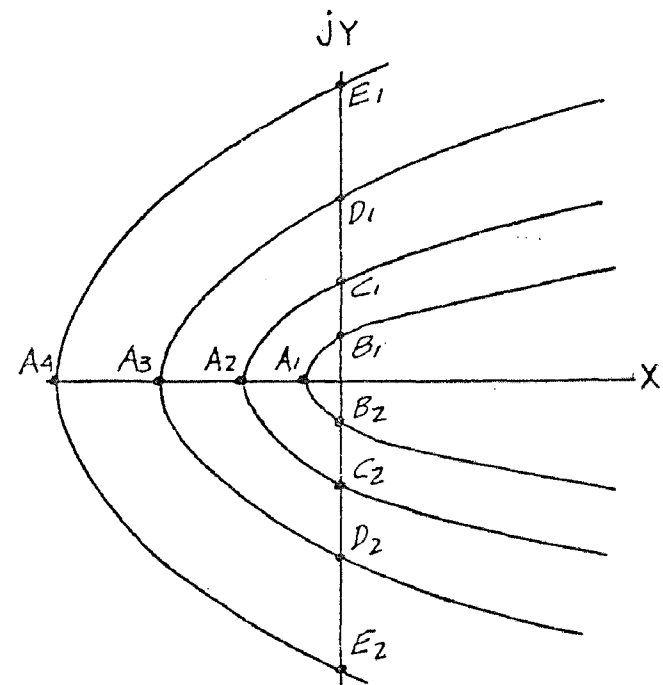
S PLANE
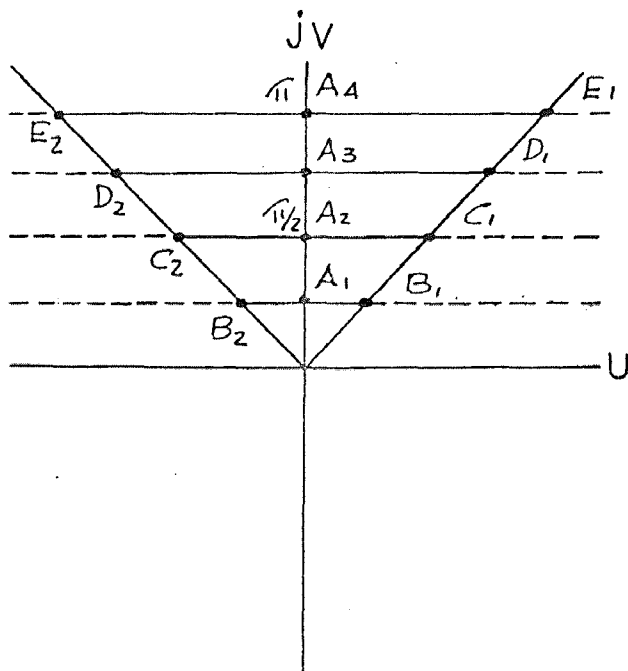
√S PLANE

NORMALIZED FOR $\tau = 1$
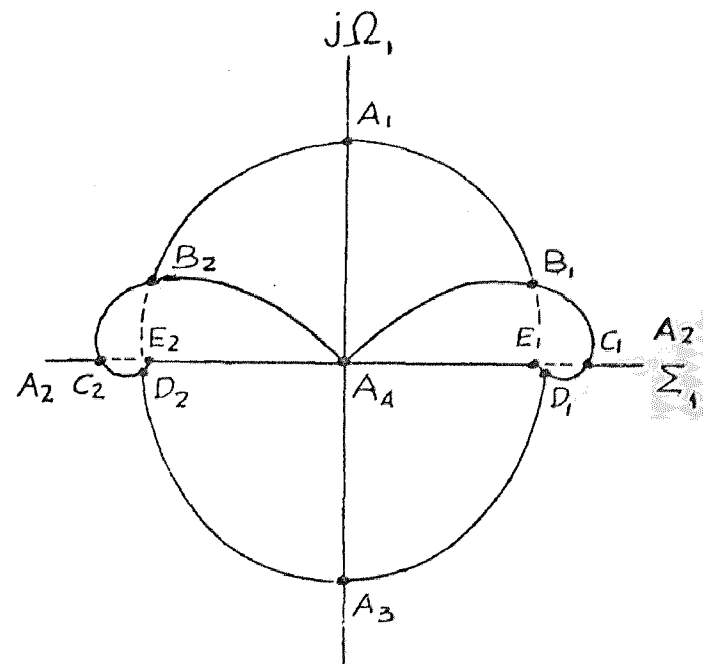
W PLANE
$W = TANH \sqrt{\tau S}$
$= \Sigma_1 + j \Omega_1$

FIGURE 5

$S \to \sqrt{S} \to W$ planes respectively. The mapping from $S \to \sqrt{S}$ plane is not conformal since, although the mapping is on a one to one basis, the angular relationships are not preserved. The $\sqrt{S} \to W$ plane mapping, however, is conformal. Figure 6 shows the several locus points which are mapped from the S-plane into the W-plane. Since the W-plane plot converges rapidly around $\sum_i = /$ (as shown in Figure 6), an expanded area about $\sum_i = /$ is shown in Figure 7.

The semi-infinite strip in the $\sqrt{S}$-plane bounded by the parallel lines $V = O$ and $V = \dfrac{\pi}{\sqrt{\tau}}$ map entirely into the W-plane. A strip twice the width, $V = \dfrac{2\pi}{\sqrt{\tau}}$, maps into the W-plane twice, once every interval $\dfrac{\pi}{\sqrt{\tau}}$. Using a normalizing constant $\sqrt{\tau}$ in Figure 8, together with Figure 9, the S-plane to W-plane transformations of the semi-infinite strips of width $\dfrac{\pi}{\sqrt{\tau}}$ are shown in Figure 10.

The information presented in Figure 6 is expanded and presented on a more accurate scale and shown in Figure 10. Using this enlarged figure, certain boundary limitations are observed.

$U = V$, which is the real frequency contour in the S-plane, is also the boundary of
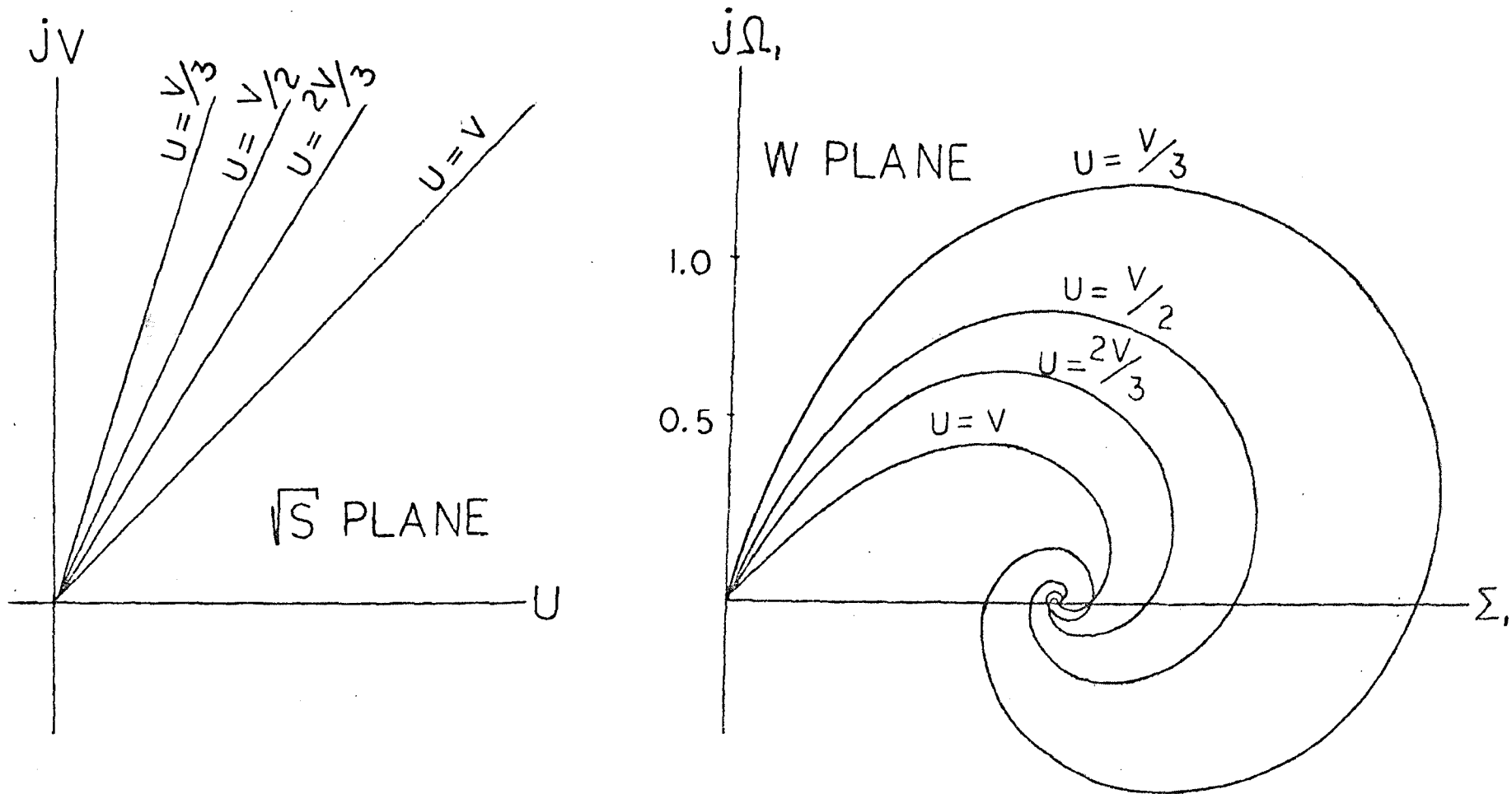
MAPPING OF LOCUS OF POINTS IN THE
√S PLANE TO THE W PLANE

FIGURE 6

EXPANDED REAL FREQUENCY
CONTOUR FOR THE VICINITY $\Sigma_1 = 1$
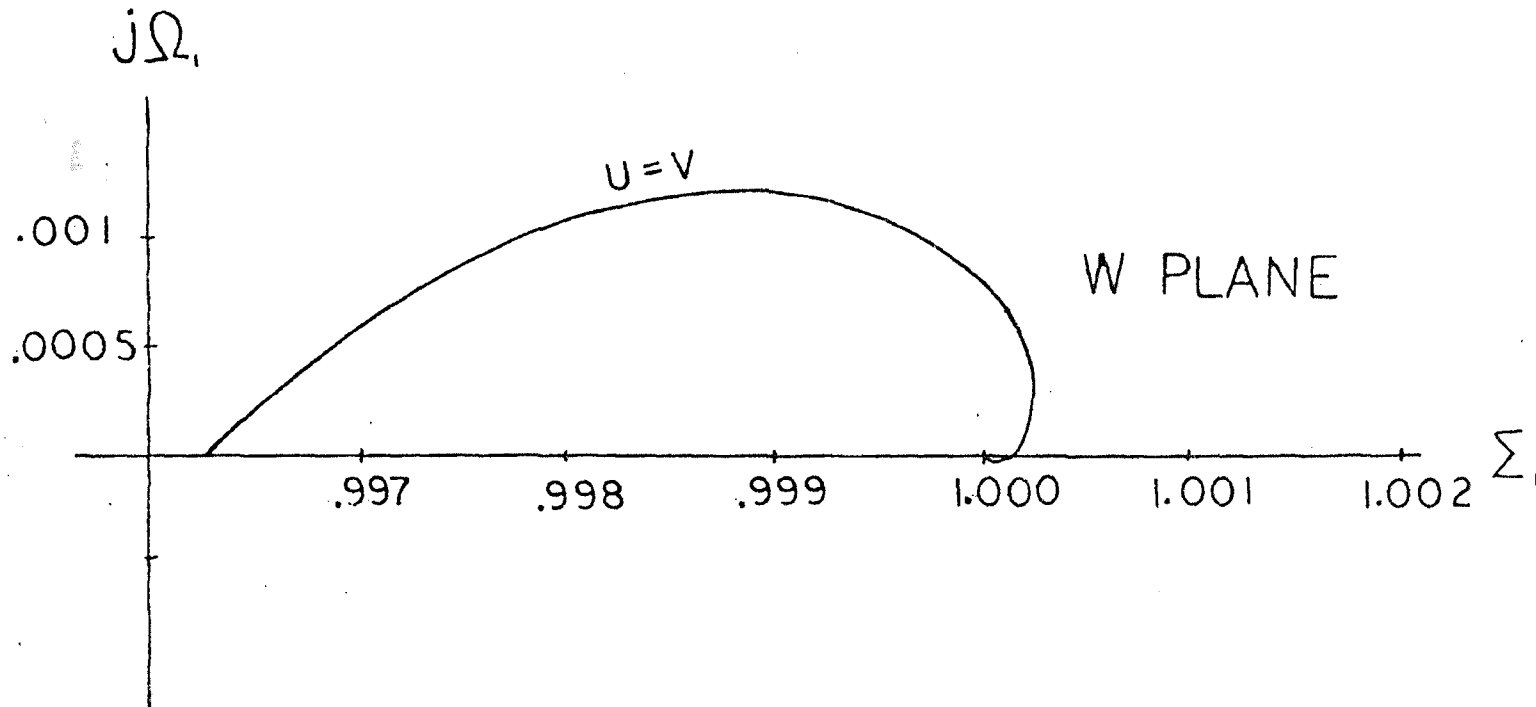
FIGURE 7

FIGURE 8
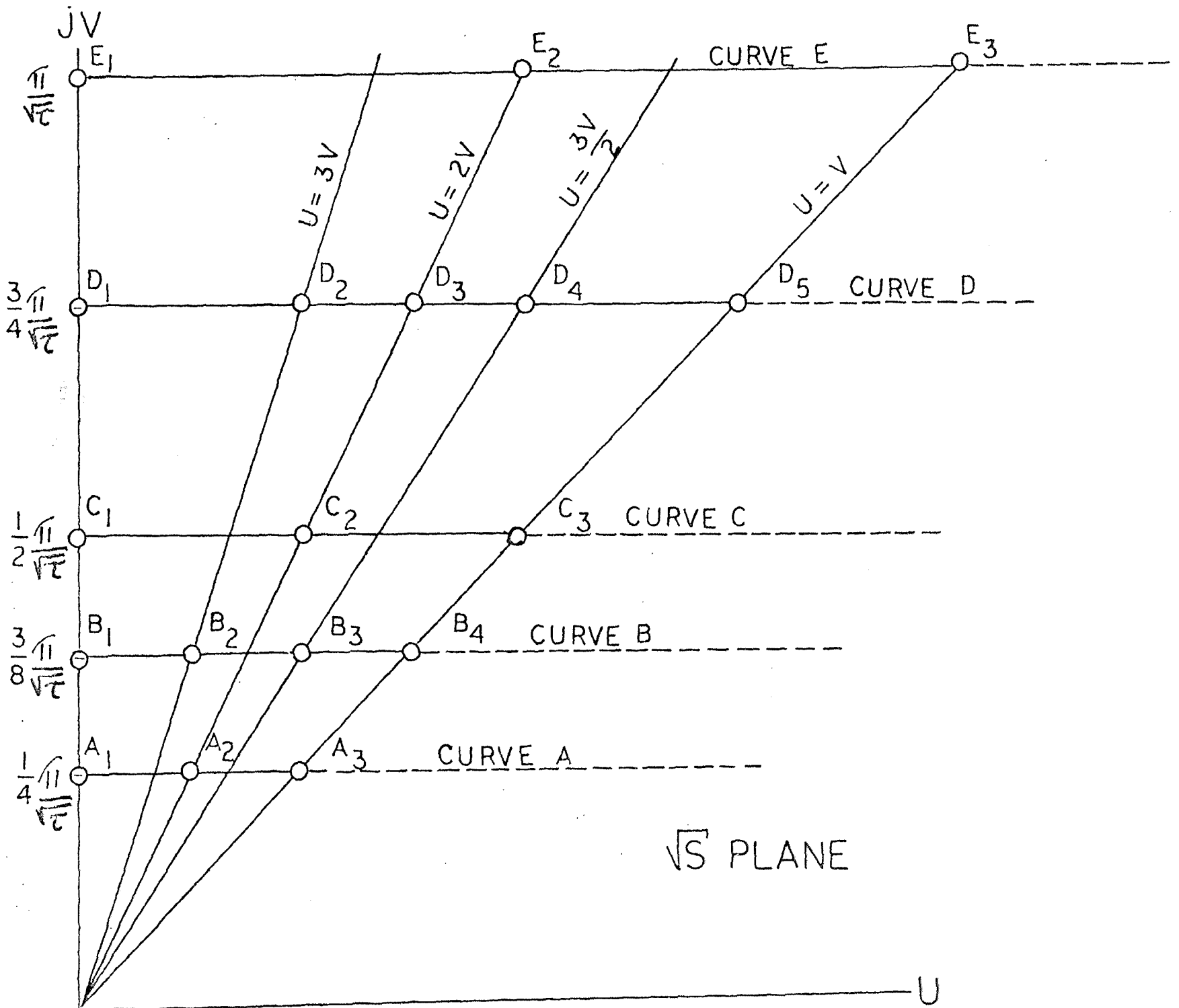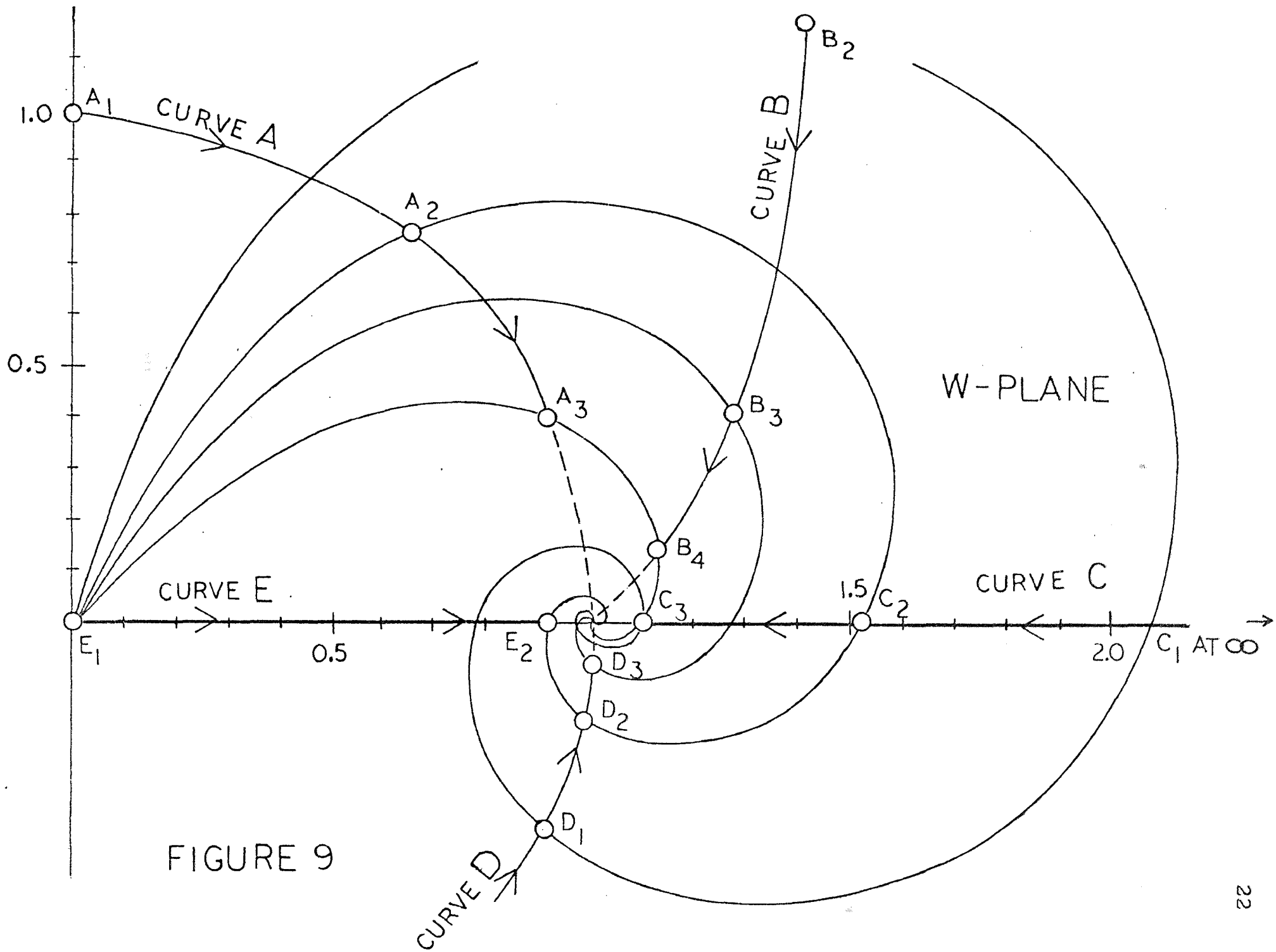
$\sqrt{S}$ PLANE

FIGURE 9

the negative real axis. Any response realization performed in the W-plane which has poles within the region bounded by the curve $U=V$ and the line extending from $\Sigma_1=O$ to $\Sigma_1=I$ is therefore unstable. Figure 10 shows the boundary limits between stable and unstable regions.

Since the $\sqrt{S}$ -plane and the W-plane are symmetrical about their imaginary axis, Figures 6 through Figures 10 consider only symmetrical half-planes. The remaining half-planes may be visualized to be mirror image figures presented about the $j\Omega_1$ axis.

W PLANE
FIGURE 10
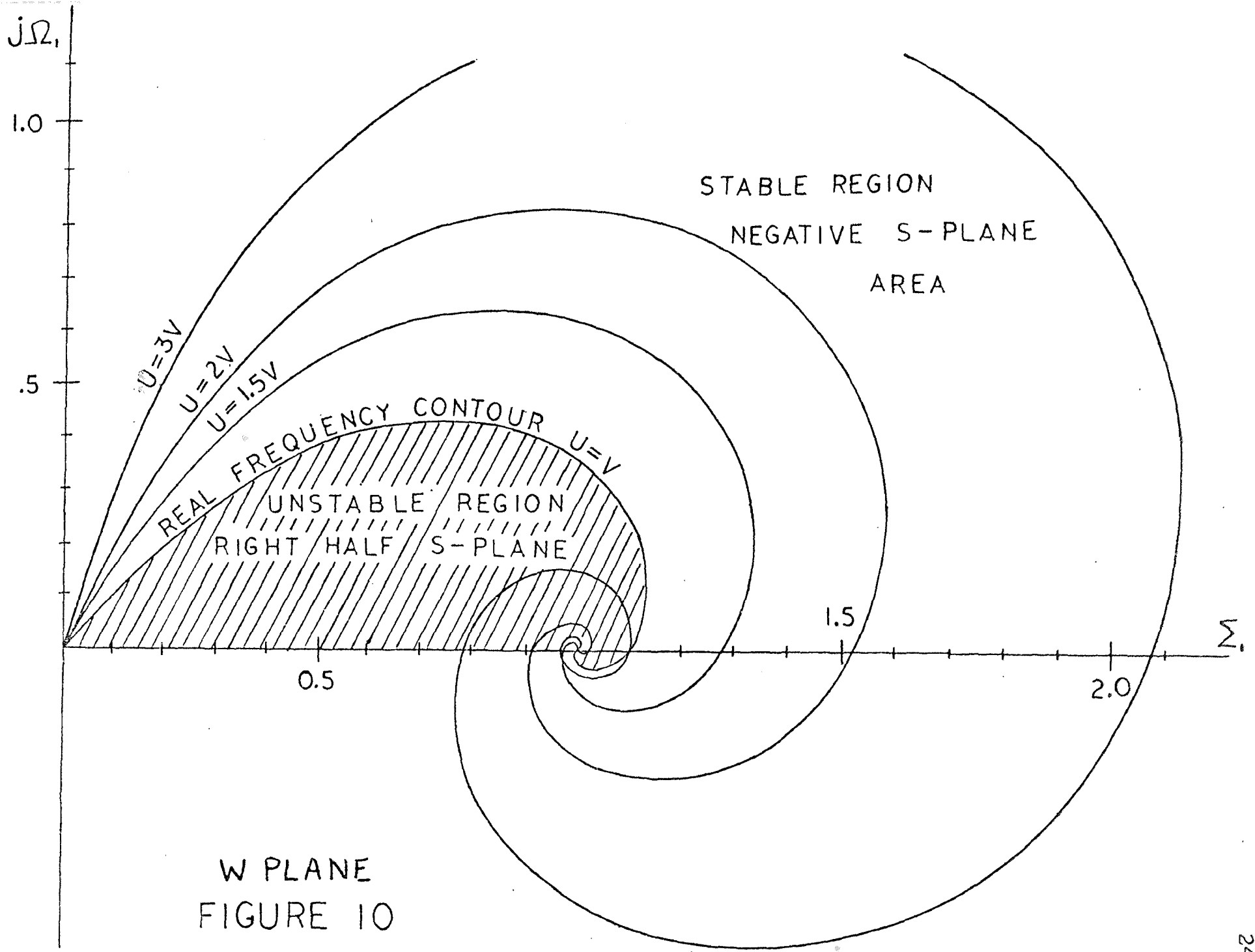
2-2   Linvill Configuration Network

The Linvill configuration[1] is composed of two
passive networks interconnected in cascade by a negative
impedance converter (NIC) as shown in Figure 11. The
general expression for the transfer function using the
Linvill configuration may be developed by multiplying
the ABCD matrices of each passive and active section
while preserving the order of multiplication. Using the
ABCD parameters of a current inversion negative impedance
converter developed in Appendix B and a general matrix
for both network N_A and N_B, the overall ABCD network
parameters are determined as

$$\begin{vmatrix} A & B \\ C & D \end{vmatrix} = \begin{vmatrix} A_1 & B_1 \\ C_1 & D_1 \end{vmatrix} \begin{vmatrix} K_1 & 0 \\ 0 & -\frac{K_1}{K_2} \end{vmatrix} \begin{vmatrix} A_2 & B_2 \\ C_2 & D_2 \end{vmatrix} \qquad (2\text{-}21)$$

The result of multiplying (2-21) is the overall matrix
for the cascaded configuration

$$\begin{vmatrix} A & B \\ C & D \end{vmatrix}_{TOTAL} = \begin{vmatrix} \left[K_1 A_1 A_2 - \frac{K_1}{K_2} B_1 C_2 \right] & \left[K_1 A_1 B_2 - \frac{K_1}{K_2} B_1 D_2 \right] \\ \left[K_1 C_1 A_2 - \frac{K_1}{K_2} D_1 C_2 \right] & \left[K_1 C_1 B_2 - \frac{K_1}{K_2} D_1 D_2 \right] \end{vmatrix}$$

$$(2\text{-}22)$$

Since interest is focused on the transfer function for
the Linvill configuration, only the ABCD to Z-parameter
transformation shall be performed to obtain the transfer
function:

LINVILL'S NETWORK CONFIGURATION
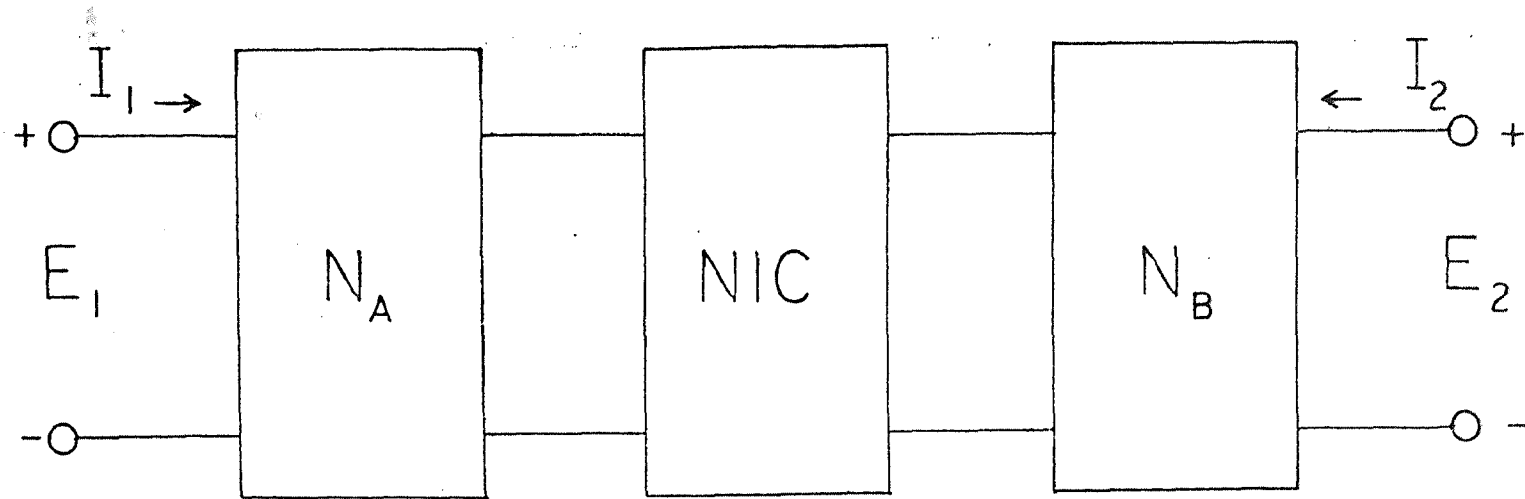
FIGURE II

$$Z_{21T} = \frac{1}{C_{TOTAL}} \qquad (2\text{-}23)$$

The expression for the transfer function via (2-22)

becomes,

$$Z_{21T} = \frac{1}{K_1 C_1 A_2 - \frac{K_1}{K_2} D_1 C_2} \qquad (2\text{-}24)$$

but

$$C_1 = \frac{1}{Z_{21}^{(A)}} \qquad (2\text{-}25a)$$

$$C_2 = \frac{1}{Z_{21}^{(B)}} \qquad (2\text{-}25b)$$

$$A_2 = \frac{Z_{11}^{(B)}}{Z_{12}^{(B)}} \qquad (2\text{-}25c)$$

$$D_1 = \frac{Z_{22}^{(A)}}{Z_{21}^{(A)}} \qquad (2\text{-}25d)$$

Replacing $Z_{12}^{(B)}$ in (2-25c) with $Z_{21}^{(B)}$ since the passive

network is reciprocal and inserting back into (2-24)

yields

$$Z_{21T} = \frac{-\frac{K_2}{K_1} Z_{21}^{(A)} Z_{21}^{(B)}}{Z_{22}^{(A)} - K_2 Z_{11}^{(B)}} \qquad (2\text{-}26)$$

If $K_2 = K$, then (2-26) becomes

$$Z_{21T} = \frac{M Z_{21}^{(A)} Z_{21}^{(B)}}{Z_{22}^{(A)} - K Z_{11}^{(B)}} \qquad (2\text{-}27)$$

where

$$\dot{M} = -\frac{K_2}{K_1} \; INIC \qquad (2\text{-}28\text{a})$$

$$M = \frac{K_2}{K_1} \; VNIC \qquad (2\text{-}28\text{b})$$

CHAPTER III.   PROPERTIES OF ACTIVE RC-NIC CASCADED

NETWORKS

3-1   Characteristics of Transfer Functions in Cascaded

RC Networks

The general expression for the transfer impedance of a Linvill network configuration was developed in section 2-2 equation (2-26) and is given again [1,12]

$$Z_{21T} = \frac{\left(\pm \frac{K_2}{K_1}\right) Z_{21}^{(A)} Z_{21}^{(B)}}{Z_{22}^{(A)} - K_2 Z_{11}^{(B)}} \tag{3-1}$$

This expression holds for any general network N_A and N_B. Identifying the networks N_A and N_B as distributed RC elements, consider the case of networks composed of single RC sections being identified as N_A and N_B shown in Figure 12. Holding the restriction $R_1^{(A)} C_1^{(A)} = R_1^{(B)} C_1^{(B)} = \tau$ remain constant, the Linvill transfer impedance using single RC elements is developed below.

The W-plane transfer and driving point impedances of a unit RC element are given below

$$Z_{11} = Z_{22} = \frac{R_1}{\sqrt{\tau} W} \tag{3-2}$$

$$Z_{21} = \frac{R_1}{\sqrt{\tau}} \frac{\sqrt{1-W^2}}{W} \tag{3-3}$$

Inserting these terms into equation (3-1) yields

$$Z_{21T}(W) = \frac{\left(\pm \frac{K_1}{K_2}\right) R_1^{(A)} R_1^{(B)} (1-W^2)}{\sqrt{\tau} \left[R_1^{(A)} - K_2 R_1^{(B)}\right] W} \tag{3-4}$$

LINVILL'S CONFIGURATION FOR REALIZATION OF TRANSFER IMMITTANCES USING $\overline{RC}$ ELEMENTS
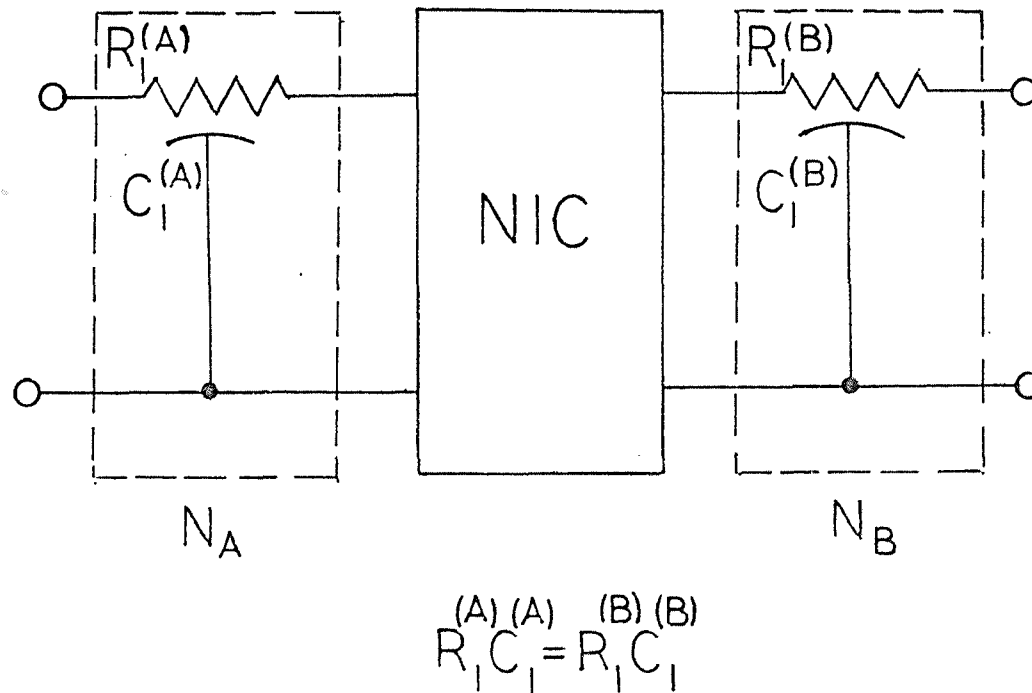
$$R_1^{(A)} C_1^{(A)} = R_1^{(B)} C_1^{(B)}$$

FIGURE 12

LINVILL'S CONFIGURATION FOR REALIZATION

OF TRANSFER IMMITTANCES USING $\overline{RC}$

ELEMENTS
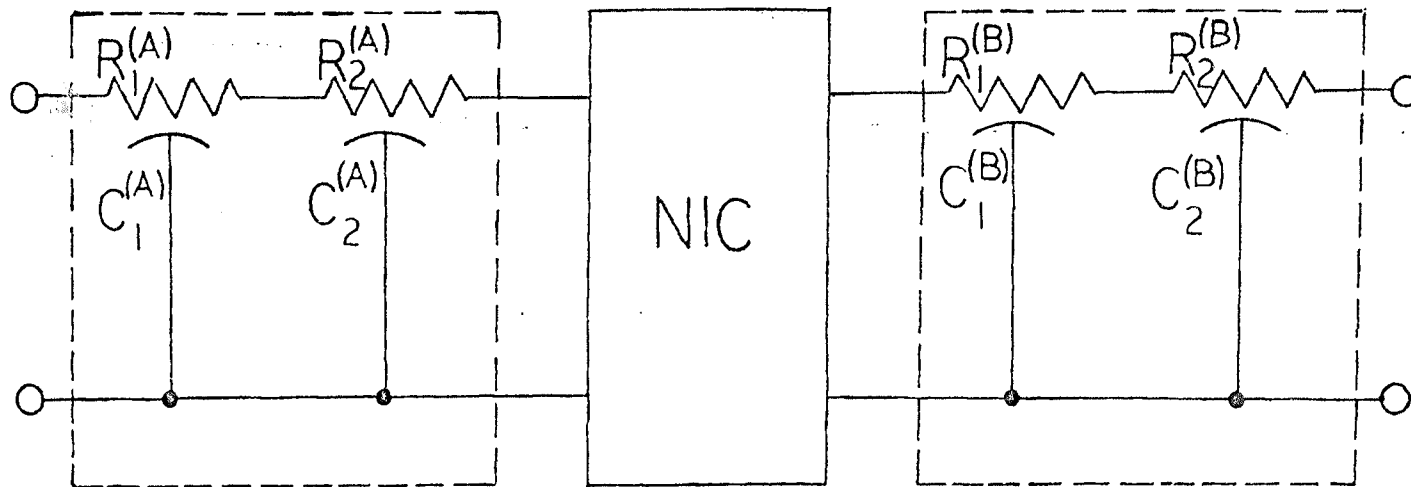
$$R_1^{(B)} C_1^{(B)} = R_1^{(A)} C_1^{(A)} = R_2^{(A)} C_2^{(A)} = R_2^{(B)} C_2^{(B)}$$

FIGURE 13

The transfer function given by (3-4) has the following singularities:

a) A W-plane pole at the origin which maps into an infinite number of interlaced poles in the S-plane.

b) Two W-plane zeros at $\sum_i = \pm /$ which correspond to transmission zeros at infinity in the S-plane.

Consider now the cascade of two $\overline{RC}$ elements in cascade contained within N_A and similarly in N_B. This cascaded $\overline{RC}$ - NIC - $\overline{RC}$ configuration is shown in Figure 13. The required expressions for the two $\overline{RC}$ elements in cascade are given below

$$Z_{11}^{(B)} = \frac{1 + \frac{R_1^{(B)}}{R_2^{(B)}} W^2}{W\left[\frac{\sqrt{C}}{R_1^{(B)}} + \frac{\sqrt{C}}{R_2^{(B)}}\right]} \qquad (3-5a)$$

$$Z_{21}^{(A)} = \frac{(1 - W^2)}{W\left[\frac{\sqrt{C}}{R_1^{(A)}} + \frac{\sqrt{C}}{R_2^{(A)}}\right]} \qquad (3-5b)$$

$$Z_{21}^{(B)} = \frac{(1 - W^2)}{W\left[\frac{\sqrt{C}}{R_1^{(B)}} + \frac{\sqrt{C}}{R_2^{(B)}}\right]} \qquad (3-5c)$$

$$Z_{22}^{(A)} = \frac{1 + \frac{R_2^{(A)}}{R_1^{(A)}} W^2}{W\left[\frac{\sqrt{C}}{R_1^{(A)}} + \frac{\sqrt{C}}{R_2^{(A)}}\right]} \qquad (3-5d)$$

Inserting the immittance expressions into (3-1) yields

$$Z_{21T}(W) = \frac{\left(\pm \frac{K_1}{K_2}\right)\left[1-W^2\right]^2}{W\left[1+\frac{R_2^{(A)}}{R_1^{(A)}}W^2\right]\left[\frac{\sqrt{\tau}}{R_1^{(B)}}+\frac{\sqrt{\tau}}{R_2^{(B)}}\right]-K_2 W\left[1+\frac{R_1^{(B)}}{R_2^{(B)}}W^2\right]\left[\frac{\sqrt{\tau}}{R_1^{(A)}}+\frac{\sqrt{\tau}}{R_2^{(A)}}\right]} \quad (3\text{-}6)$$

Using the following substitutions in (3-6)

$$\beta_1^{(A)} = \frac{R_2^{(A)}}{R_1^{(A)}} \quad (3\text{-}7a)$$

$$\beta_1^{(B)} = \frac{R_1^{(B)}}{R_2^{(B)}} \quad (3\text{-}7b)$$

$$K^{(A)} = \frac{\sqrt{\tau}}{R_1^{(A)}} + \frac{\sqrt{\tau}}{R_2^{(A)}} \quad (3\text{-}7c)$$

$$K^{(B)} = \frac{\sqrt{\tau}}{R_1^{(B)}} + \frac{\sqrt{\tau}}{R_2^{(B)}} \quad (3\text{-}7d)$$

results in a simplification of (3-6) after slight

manipulation

$$Z_{21T}(W) = \frac{\left(\pm \frac{K_2}{K_1}\right)\left(1-W^2\right)^2}{W\left[\beta_1^{(A)}K^{(B)}-K_2\beta_1^{(B)}K^{(A)}\right]\left[\frac{K^{(B)}-K_2 K^{(A)}}{\beta_1^{(A)}K^{(B)}-K_2\beta_1^{(B)}K^{(A)}}+W^2\right]} \quad (3\text{-}8)$$

In general (3-8) may be written as

$$Z_{21T}(W) = \frac{M\left(1-W^2\right)^2}{W\left[W^2 \pm Q^2\right]} \quad (3\text{-}9)$$

where

$$M = \frac{\left(\pm \frac{K_2}{K_1}\right)}{\beta_1^{(A)}K^{(B)}-K_2\beta_1^{(B)}K^{(A)}} \quad (3\text{-}10)$$

and

$$Q = \frac{K^{(A)}}{\beta_1^{(B)} K^{(A)}} \sqrt{\frac{\dfrac{K^{(B)}}{K^{(A)}} - K_2}{\dfrac{\beta_1^{(A)} K^{(B)}}{\beta_1^{(B)} K^{(A)}} - K_2}} \qquad (3\text{-}11)$$

are real constants.

In equation (3-11), Q may be either positive or negative depending on the sign of K_2, the negative impedance conversion ratio, and due to the difference term, the magnitude of K_2 will also alter the sign of (3-11). It is for this reason that the numerator in (3-9) contains the $\pm$ term.

The S-plane pole solutions to (3-9) are derived in Appendix C. For the case when the W-plane transfer impedance is of the form

$$Z_{21T}(w) = \frac{M(1-w^2)^2}{w(w^2+Q_1^2)} \qquad (3\text{-}12)$$

This corresponds to the S-plane transfer impedance given by

$$Z_{21T}(\sqrt{s'}) = \frac{M}{\sinh\sqrt{\tau s'}\,\cosh^3\sqrt{\tau s'}\,(\tanh^2\sqrt{\tau s'}+Q_1^2)} \qquad (3\text{-}13)$$

the singularities of which are located at points

$$S = -\frac{(m+\frac{1}{2})^2 \pi^2}{\tau}, \quad n = 0,1,2,\cdots \qquad (3\text{-}14\text{a})$$

$$S = -\frac{m^2 \pi^2}{\tau}, \quad n = 0,1,2,\cdots \qquad (3\text{-}14\text{b})$$

$$S = -\frac{1}{4\tau}\left[2\pi r_1 + 2\tan^{-1}Q_1\right]^2, \quad \begin{array}{l} r_1 = 0,1,2,\ldots \\ n = 0,1,2,\ldots \end{array} \quad (3\text{-}14c)$$

$$S = -\frac{1}{4\tau}\left[\pi r_2 + 2\tan^{-1}Q_1\right]^2 \quad \begin{array}{l} r_2 = 1,2,\ldots \\ n = 0,1,2,\ldots \end{array} \quad (3\text{-}14d)$$

where the poles given by (3-14a) are third order poles.

From equation (3-14) we see that no complex S-plane pole solutions exist, therefore this selection of circuit constants which provide positive Q

i.e. $\left[\dfrac{\dfrac{K^{(B)}}{K^{(A)}} - K_2}{\dfrac{B_1^{(A)}K^{(B)}}{B_1^{(B)}K^{(A)}} - K_2}\right]^{\frac{1}{2}}$ is positive do not permit

shaping of the transfer function by manipulating pole positions since all the poles are restricted to the negative real S-plane axis.

A more interesting case exists when Q is negative, under this condition the W-plane transfer function given by (3-12) becomes

$$Z_{2/T}(W) = \frac{M}{W(W^2 - Q_2^2)} \quad (3\text{-}15)$$

The corresponding $\sqrt{S}$-plane transfer function is given by

$$Z_{2/T}(\sqrt{S}) = \frac{M}{\sinh\sqrt{\tau S}\cosh^3\sqrt{\tau S}(\tanh^2 - Q_2^2)} \quad (3\text{-}16)$$

for which the S-plane pole solutions are

$$S = -\frac{(m+\frac{1}{2})^2\pi^2}{\tau} \quad m = 0,1,2,\ldots \quad (3\text{-}17a)$$

$$S = -\frac{n^2 \pi^2}{\tau} \qquad n = 0, 1, 2, \ldots \qquad (3\text{-}17b)$$

$$S = \frac{1}{4\tau}\left[-\log_e\left|\frac{1-Q_2}{1+Q_2}\right| + j\left(\pi[r_3+1] - \phi\right)\right]^2, \quad \begin{array}{l} r_3 = 1, 2, \ldots \\ \phi = K\pi \\ K = 0, 1, 2, \ldots \end{array} \qquad (3\text{-}17c)$$

$$S = \frac{1}{4\tau}\left[-\log_e\left|\frac{1+Q_2}{1-Q_2}\right| - j\left(\pi r_4 - \phi\right)\right] \quad \begin{array}{l} r_4 = 0, 1, 2, \ldots \\ \phi = K\pi \\ K = 0, 1, 2, \ldots \end{array} \qquad (3\text{-}17d)$$

The S-plane solutions of (3-17) do provide complex pole pairs in the transfer function.

3-2 Realization of Pole Pairs via Linvill Configuration

The Linvill network configuration for realization of transfer impedances using cascaded $\overline{RC}$ elements can provide the following W-plane pole roots:

a) Zeros of higher order at the points $\sum = \pm 1$ depending upon the number of cascaded sections under consideration.

b) A pole at the origin, independent of the number of sections under consideration.

c) A conjugate pair of poles either on the imaginary W-plane axis or the real W-plane axis due to the difference term in the denominator of the transfer impedance.

Due to the network configuration, one of two possible cases may evolve:

a) $\beta_1^{(B)}$ is greater than $\beta_1^{(A)}$ (ref. equation (3-7) sec. 3-1). Under this condition when the NIC conversion ratio K_2 is zero, the roots lie at points $A \notin A'$, see Figure 14. As the conversion ratio K_2 approaches $\dfrac{\beta_1^{(A)} K^{(B)}}{\beta_1^{(B)} K^{(A)}}$ the poles approach $\pm$ infinity, along the imaginary W-plane axis. When $\dfrac{\beta_1^{(A)} K^{(B)}}{\beta_1^{(B)} K^{(A)}} K_2 < \dfrac{K^{(B)}}{K^{(A)}}$ the poles lie on the real axis and are at the origin when $K_2 = \dfrac{K^{(B)}}{K^{(A)}}$. For $K_2 > \dfrac{K^{(B)}}{K^{(A)}}$ the poles are on the imaginary axis and approach $B \notin B'$ in the limit.

POLE PAIR LOCATIONS FOR LINVILL'S SYNTHESIS
USING CASCADED $\overline{RC}$ SECTIONS
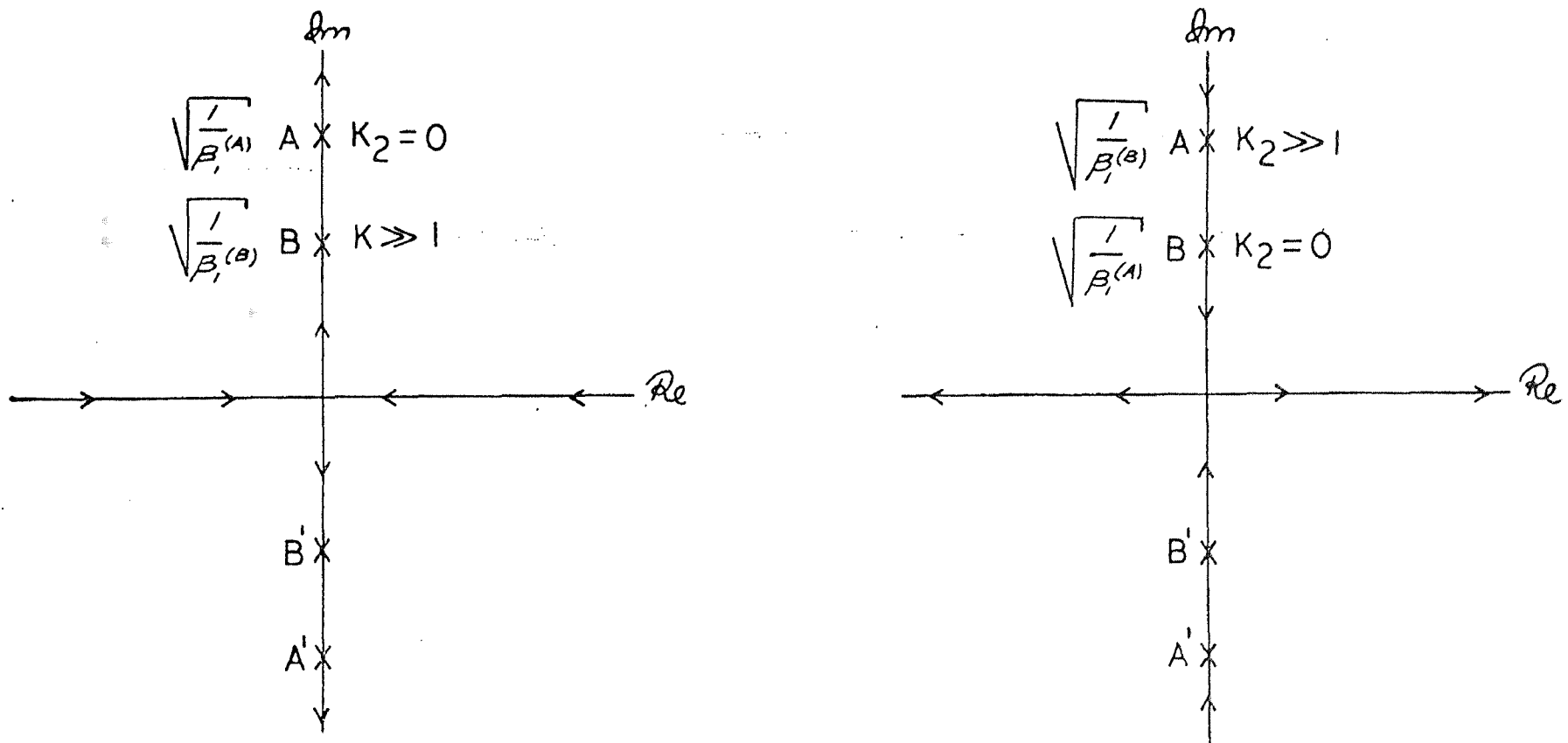
FIGURE 14

b) $\beta_1^{(A)}$ is reater then $\beta_1^{(B)}$. Under this condition when the NIC conversion ratio K_2 is zero, the poles lie at $B \& B'$, see Figure 14. As the conversion ratio K_2 approaches $\dfrac{K^{(B)}}{K^{(A)}}$ the poles approach the ori;in. When $\dfrac{K^{(B)}}{K^{(A)}} < K_2 < \dfrac{\beta_1^{(A)} K^{(B)}}{\beta_1^{(B)} K^{(A)}}$ the poles lie on the positive and negative real W-plane axis and approach infinity as $K_2 \rightarrow \dfrac{\beta_1^{(A)} K^{(B)}}{\beta_1^{(B)} K^{(A)}}$. For $K_2 > \dfrac{\beta_1^{(A)} K^{(B)}}{\beta_1^{(B)} K^{(A)}}$, the poles appear on the imaginary axis and approach the points $A \& A'$ as K_2 gets very large.

The case when the W-plane pole locations lie on the imaginary axis corresponds to the negative real axis S-plane poles and is of no interest since shaping of the transfer impedance is not possible.

When the W-plane pole locations exist on the real axis, complex S-plane pole solutions are obtained. Precaution should be taken since RH S-pole solutions are also possible.

THEOREM I. A sufficient condition for the realization of a transfer impedance with complex poles using cascaded $\overline{RC}$ elements in a Linvill configuration is that the W-plane poles lie on the real axis at points not less than 1.0903 .

THEOREM II. A transfer function with S-plane poles
in the LHP can be realized using cascaded
$\overline{RC}$ elements in a Linvill configuration.

3-3 Example of the Linvill RC Network Configuration

Consider the example shown in Figure 15. The time constant for the network is $\tau = 3$. Using the values given in Figure 15 and substituting into equation (3-7) section 3-1 yields

$$\beta_1^{(A)} = 0.468 \tag{3-18a}$$

$$\beta_1^{(B)} = 29.2 \tag{3-18b}$$

$$K^{(A)} = 0.936 \tag{3-18c}$$

$$K^{(B)} = 12.51 \tag{3-18d}$$

inserting these values into equation (3-8) section 3-1 yields

$$Z_{21T}(w) = \left(-\frac{K_2}{K_1}\right)\left(\frac{1}{5.82 - 27.3 K_2}\right)\left[\frac{(1-w^2)^2}{w\left[w^2 + \left(\sqrt{\frac{12.51 - 0.936 K_2}{5.82 - 27.3 K_2}}\right)^2\right]}\right] \tag{3-19}$$

Using Figure 10, it is seen that the real frequency contour intersects the W-plane real axis at $\Sigma = \pm 1.0903$ which represents the boundary between the region of stability and instability.   Poles on the real W-plane axis located at points less than $\Sigma = 1.0903$ correspond to poles in the RH S-plane.

The value of K_2 which provides the value for $Q_2 = \sqrt{1.0903}$ is found to be $K_2 = 0.614$. Choose $K_1 = 1$; then the total expression becomes

$$Z_{21T}(w) = \frac{0.056 (1-w^2)^2}{w\left[w^2 + \left(\sqrt{-1.0903}\right)^2\right]} \tag{3-20}$$

EXAMPLE OF LINVILL'S CONFIGURATION FOR

REALIZATION OF TRANSFER IMMITTANCE USING

TWO $\overline{RC}$ CASCADES
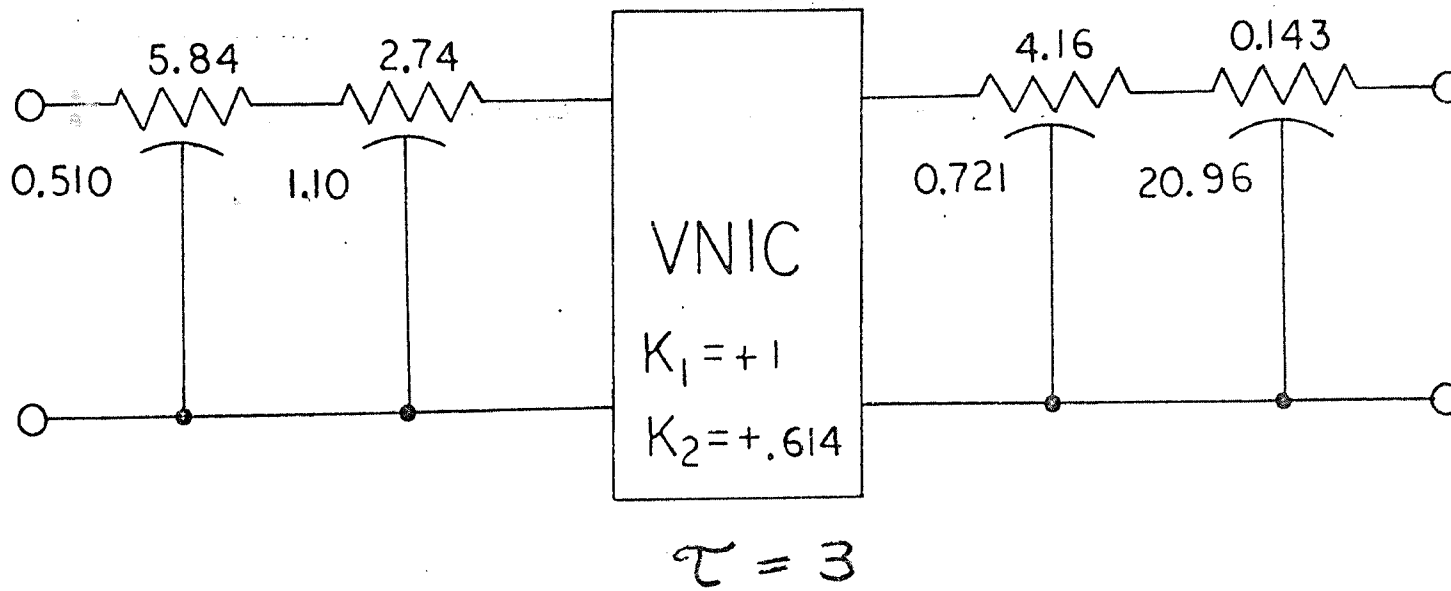
ALL VALUES IN OHMS OR FARADS

FIGURE 15

S-PLANE POLE LOCATIONS FOR

$$Z_{21}(S) = \frac{0.056}{\text{SINH}\sqrt{3S}\ \text{COSH}^3\sqrt{3S}\ (\text{TANH}^2 - Q^2)}$$

FIRST AXIS POLE
AT $\Pi^2/4\tau$

(3)

$\tau = 3$

Q = 1.15

Q = 1.12

Q = 1.10

Q = 1.0903

$\frac{5}{\tau}$

$\frac{1}{\tau}$

$\frac{0.5}{\tau}$

$\frac{0.1}{\tau}$

$-\frac{5}{\tau}$
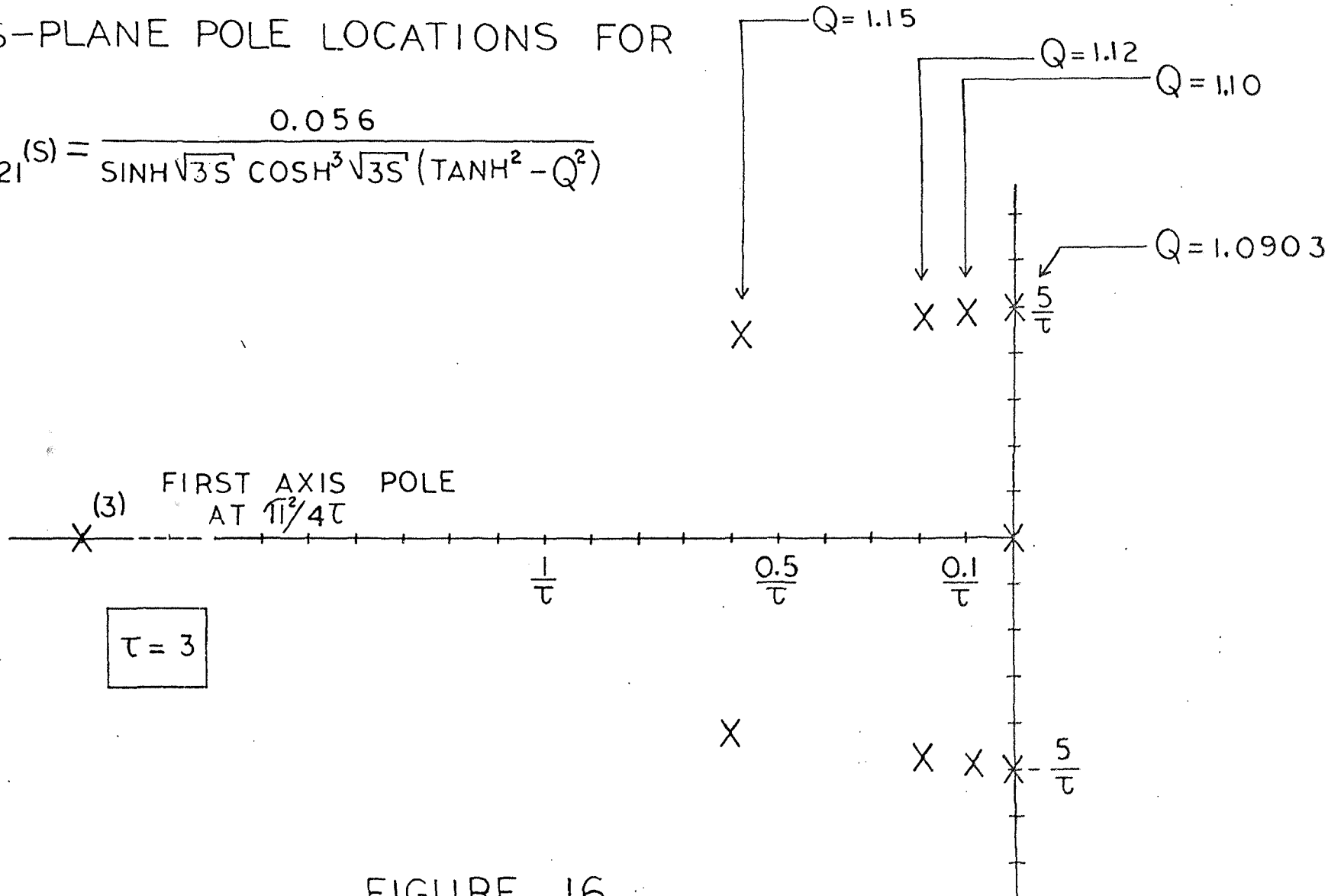
FIGURE 16

The roots of equation (3-20) are located at the following points in the S-plane

and

$$S = 0, \quad -\frac{\pi^2}{4\tau}, \quad \frac{\pi^2}{\tau}, \quad -\frac{9\pi^2}{4\tau}, \quad \cdots$$

$$S = \pm j\frac{\pi^2}{2\tau}, \quad \pm j\frac{3\pi^2}{2\tau}, \quad \pm j\frac{5\pi^2}{2\tau}, \quad \cdots$$

The root locations are on the imaginary axis since the limiting value of $Q = 1.0903$ was used. For the case when the value of Q is greater than 1.0903, the S-plane root pairs become complex as shown in Figure 16.

A computer plot, Figure 17, is obtained by letting $S = j\omega$ and the response is presented in db form. The zero line is used as reference where the transfer function is unity. In actuality however, the value of M in section 3-1 equation (3-9) is not unity but $.056\sqrt{\tau}$ which represents a shift of -20.2 db. The response of the example is plotted over two decades in terms of the normalized units $\dfrac{\pi^2}{2RC}$.

FIGURE 17

RADIANT FREQ. IN UNITS OF $\dfrac{\pi^2}{2RC}$

Q=1.10

Q=1.12

Q=1.15
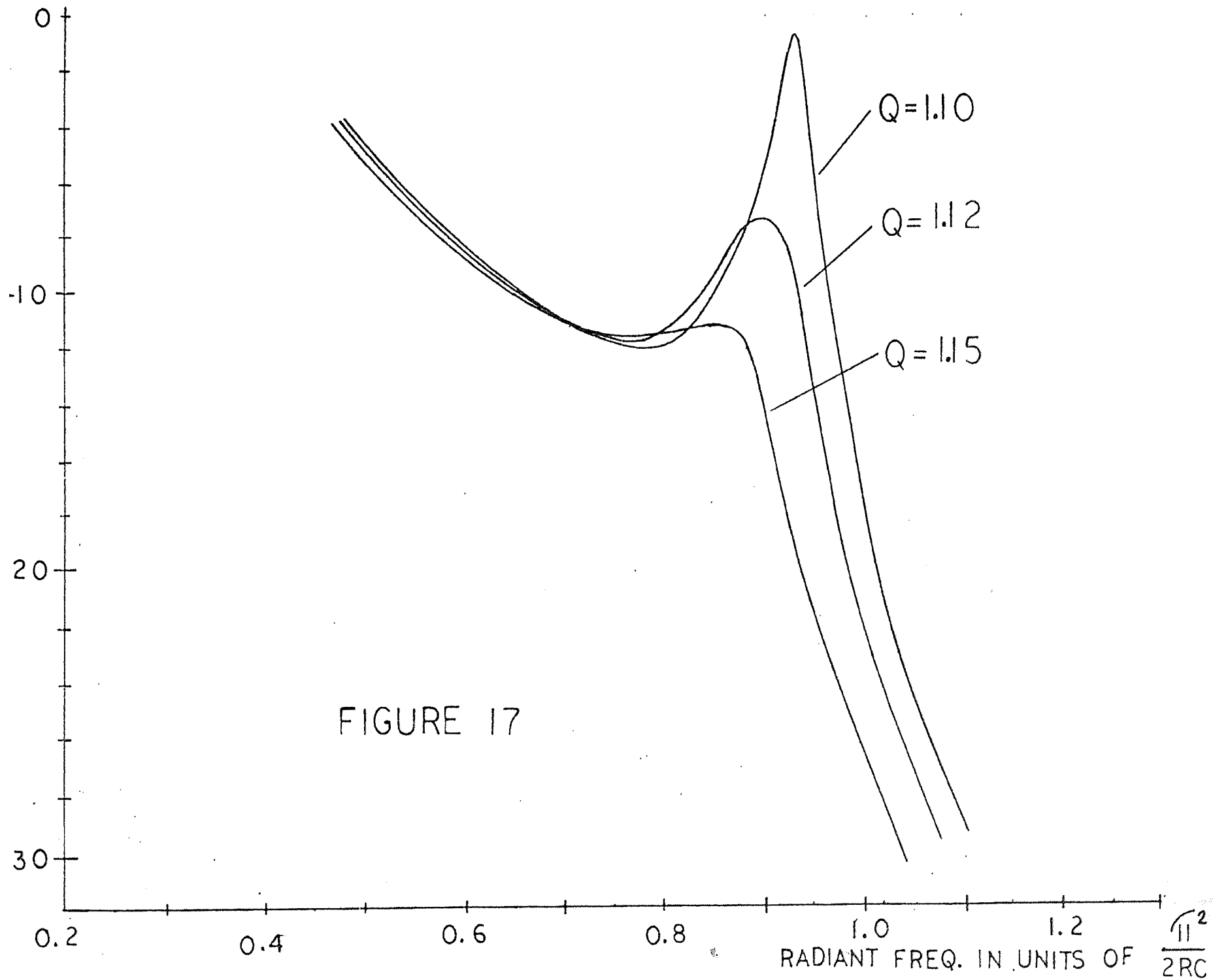
CHAPTER IV.   CONCLUSION

4-1   Summary of Results

The negative impedance converter in the Linvill configuration is an effective active element in producing complex poles in the transfer function $Z_{2/T}$ when the passive networks are $\overline{RC}$ cascades who by themselves do not posses complex S-plane poles.

The pole producing term in the W-plane $Z_{2/T}$ function is $\left(W^2 - Q_1^2 \right)$, which produce LHP poles in the S-plane with the restriction $Q_1 > 1.0903$. For $Q_1 < 1.0903$ the poles are in the RHP and the response becomes unstable.

The transfer impedance generated via the Linvill procedure using only cascaded $\overline{RC}$ elements contains an S-pl pole at the origin. This prevents the synthesis of band-pass filters employing only $\overline{RC}$ cascades without the use of shunt stubs. This limitation of the circuit is not so serious since the voltage transfer ratio for the configuration shown in Figure 13 does not contain any poles at the origin in the S-plane.

4-2   Suggestions for Future Work

Since a variety of network synthesis procedures have been developed, the boundary limitations for realizability and stability are not necessarily included

in the development of such procedures. A similar procedure used in this thesis should be extended to other configurations to determine the limitations of realizability criteria and to identify the boundaries of stability.

An extension of the cascaded RC elements to cascaded and shunt (stubs) RC elements in the Linvill configuration is suggested.

APPENDIX A

Consider Wyndrum's positive real transformation[8]

$$S_1(\sqrt{S}) = \tanh \frac{a}{2}\sqrt{S} = \Sigma_1 + j\Omega_1 \tag{1}$$

where the coordinates in the $\sqrt{S}$ plane are $U+jV$.
Using the substitution for $\tanh$ and letting $\sqrt{S} = U+jV$
equation (1) becomes

$$\tanh \frac{a}{2}\sqrt{S} = \frac{\sinh\left(\frac{a}{2}U + j\frac{a}{2}V\right)}{\cosh\left(\frac{a}{2}U + j\frac{a}{2}V\right)} \tag{2}$$

$$\tanh \frac{a}{2}\sqrt{S} = \frac{\sinh\left(\sqrt{\tau}U + j\sqrt{\tau}V\right)}{\cosh\left(\sqrt{\tau}U + j\sqrt{\tau}V\right)} \tag{3}$$

expanding (3) yields,

$$\tanh\sqrt{\tau S} = \frac{\sin\sqrt{\tau}U \cosh j\sqrt{\tau}V + \sinh j\sqrt{\tau}V \cosh\sqrt{\tau}U}{\cosh\sqrt{\tau}U \cosh j\sqrt{\tau}V + \sinh j\sqrt{\tau}V \sinh\sqrt{\tau}U} \tag{4}$$

Substituting $\sinh j\Theta = j\sin\Theta$ and $\cosh j\Theta = \cos\Theta$
into (4) and multiplying through by the conjugate of the
denominator yields equation (5) after simplification
and identification of terms.

$$\tanh \sqrt{zs} = \frac{\sinh\sqrt{z}\, U \cosh\sqrt{z}\, U + j \sin\sqrt{z}\, V \cos\sqrt{z}\, V}{\cos^2\sqrt{z}\, V + \sinh^2\sqrt{z}\, U} \tag{5}$$

The coordinates of the $\tanh$ plane in terms of the coordinates of the $\sqrt{s}$ plane are given by (6) and (7) below

$$\Sigma_1 = \frac{\sinh\sqrt{z}\, U \cosh\sqrt{z}\, U}{\cos^2\sqrt{z}\, V + \sinh^2\sqrt{z}\, U} \tag{6}$$

$$\Omega_1 = \frac{\sin\sqrt{z}\, V \cos\sqrt{z}\, V}{\cos^2\sqrt{z}\, V + \sinh^2\sqrt{z}\, U} \tag{7}$$

Equations (6) and (7) provide the required transformation from the distributed LC plane to the lumped LC plane.

APPENDIX B

The ideal negative-impedance converter[7] is an active two-port device with the property that the driving point impedance or admittance at one terminal pair is the negative of the impedance or admittance connected at the other terminal pair.

The description of the NIC properties are obtained by considering the relationship between the terminal voltages and the currents of the two-port device. Consider the two-port shown below;
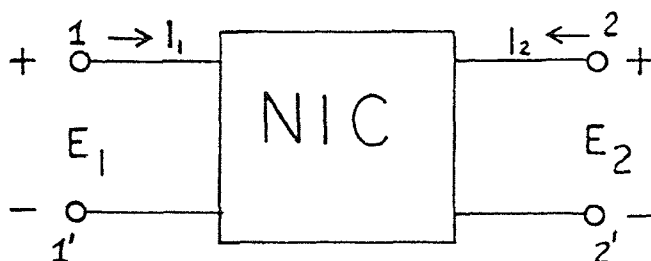
where the voltage and current interrelationships are given by the hybrid g parameters

$$
\begin{vmatrix} I_1 \\ E_2 \end{vmatrix} = \begin{vmatrix} g_{11} & g_{12} \\ g_{21} & g_{22} \end{vmatrix} \begin{vmatrix} E_1 \\ I_2 \end{vmatrix} \tag{1}
$$

The input admittance $\dfrac{I_1}{E_1}$ at terminals 1-1' is given by

$$
\frac{I_1}{E_1} = Y_{IN(1-1')} = g_{11} - \frac{g_{12}\, g_{21}}{g_{22} + Z_L} \tag{2}
$$

For an ideal NIC,

$$Y_{IN(I-I')} = -\frac{1}{Z_L} \tag{3}$$

This can only be obtained if

$$g_{II} = O \tag{4}$$

$$g_{22} = O \tag{5}$$

and

$$g_{I2} \, g_{2I} = I \tag{6}$$

Inserting these values of the hybrid parameters into equation (1) yields

$$\begin{vmatrix} I_I \\ E_2 \end{vmatrix} = \begin{vmatrix} O & I \\ I & O \end{vmatrix} \begin{vmatrix} E_I \\ I_2 \end{vmatrix} \tag{7}$$

Since the Linvill configuration consists of elements in cascade, the ABCD parameters are more useful and shall be developed to express the NIC characteristics. Using the transformation given below

$$\begin{vmatrix} A & B \\ C & D \end{vmatrix} = \begin{vmatrix} \dfrac{I}{g_{2I}} & \dfrac{g_{22}}{g_{2I}} \\ \dfrac{g_{II}}{g_{2I}} & \dfrac{\Delta g}{g_{2I}} \end{vmatrix} \tag{8}$$

the ABCD parameters are identically

$$A = \frac{I}{g_{2I}} \tag{9-a}$$

$$B = O \tag{9-b}$$

$$C = 0 \tag{9-c}$$

$$D = - g_{12} \tag{9-d}$$

There two types of negative impedance converters, current inversion negative impedance converter INIC and voltage inversion negative impedance converter VNIC. The ABCD parameters for an INIC are given by equation (9), and the ABCD parameters for a VNIC are given below

$$
\begin{vmatrix} A & B \\ C & D \end{vmatrix} = \begin{vmatrix} \dfrac{1}{g_{21}} & 0 \\ 0 & g_{12} \end{vmatrix} \tag{10}
$$

In order to standardize on the notation for the NIC with the notation used in the Linvill configuration, the following substitutions shall be made,

$$g_{12} \, g_{21} = \frac{1}{K_2} \tag{11}$$

$$\frac{1}{g_{21}} = K_1 \tag{12}$$

The generalized ABCD parameters for a NIC using the notation of (11) and (12) are

$$
\begin{vmatrix} A & B \\ C & D \end{vmatrix} = \begin{vmatrix} K_1 & 0 \\ 0 & \pm \dfrac{K_1}{K_2} \end{vmatrix} \tag{13}
$$

where the D term may be either positive (VNIC) or negative (INIC).

APPENDIX C

The equation for the transfer impedance using a cascade of two RC sections per network in the Linvill configuration shown in Figure 13 is of the form

$$Z_{2IT_{LC}}(W) = \frac{M(1-W^2)^2}{W(W^2 \pm Q_1^2)} \tag{1}$$

where Q_1 is real.

Using the transformation $W = \tanh\sqrt{\zeta s}$ to transform (1) from the lumped LC plane to the distributed LC plane yields

$$Z_{2IT_{LC}}(\sqrt{s}) = \frac{M}{\sinh\sqrt{\zeta s}\ \cosh^3\sqrt{\zeta s}\ (\tanh^2\sqrt{\zeta s} \pm Q^2)} \tag{2}$$

where the roots of $\cosh\sqrt{\zeta s}$ are

$$\sqrt{s} = j\frac{(n+\frac{1}{2})\pi}{\sqrt{\zeta}} \qquad n = 0, 1, 2, \ldots \tag{3}$$

and the roots of $\sinh\sqrt{\zeta s}$ are

$$\sqrt{s} = j\frac{n\pi}{\sqrt{\zeta}} \qquad n = 0, 1, 2, \ldots \tag{4}$$

To evaluate the roots of $\tanh^2\sqrt{\zeta s} \pm Q^2$, it is observed that two possible root pairs exist,

$$\tanh^2\sqrt{\zeta s} + Q_1^2 = 0 \tag{5}$$

and

$$\tanh^2\sqrt{\zeta s} - Q_2^2 = 0 \tag{6}$$

Consider the first possible root pairs

$$\tanh^2 \sqrt{\tau s} + Q_1^2 = 0 \qquad (7)$$

Equation (7) is composed of the following produst terms,

$$\left(\tanh \sqrt{\tau s} + j\, Q_1\right)\left(\tanh \sqrt{\tau s} - j\, Q_1\right) = 0 \qquad (8)$$

Consider the roots of the first term of (8)

$$\tanh \sqrt{\tau s} = -j\, Q_1 \qquad (9)$$

using the identity $\tanh \sqrt{\tau s} = \dfrac{\sinh \sqrt{\tau s}}{\cosh \sqrt{\tau s}}$ equation (9) becomes

$$\sinh \sqrt{\tau s} = -j\, Q_1 \cosh \sqrt{\tau s} \qquad (10)$$

or

$$e^{\sqrt{\tau s}} - e^{-\sqrt{\tau s}} = j\, Q_1 \left[e^{\sqrt{\tau s}} + e^{-\sqrt{\tau s}} \right] \qquad (11)$$

regrouping terms

$$-\left(1 + j\, Q_1\right) e^{\sqrt{\tau s}} + \left(1 - j\, Q_1\right) e^{-\sqrt{\tau s}} = 0 \qquad (12)$$

dividing both sides by $\left(1 - j\, Q_1\right) e^{-\sqrt{\tau s}}$ yields

$$1 = \left(\frac{1 + j\, Q_1}{1 - j\, Q_1}\right) e^{2\sqrt{\tau s}} \qquad (13)$$

but

$$\left(\frac{1 + j\, Q_1}{1 - j\, Q_1}\right) = \left| \frac{1 + j\, Q_1}{1 - j\, Q_1} \right| e^{j\left(2\tan^{-1} Q_1 + 2m\pi\right)} \qquad (14\text{-a})$$

$$\left(\frac{1+j\Theta_1}{1-j\Theta_1} \right) = e^{(j\,2\,tau\,\Theta_1\,+\,j\,2m\pi\,)} \qquad (14\text{-}b)$$

since Θ_1 is real.

Inserting back into (13) yields

$$1 = \left[e^{j\,2\,tau^{-1}\Theta_1\,+\,j\,2m\pi} \right] e^{2\sqrt{\tau s}} \qquad (15)$$

but

$$1 = e^{j\,2n\pi} \qquad (16)$$

therefore

$$2\sqrt{\tau s} = j\,2\pi r_1 - j\,2\,tau^{-1}\Theta_1 \qquad (17)$$

where $r_1 = (n-m)$

The roots contributed by (17) lie on the imaginary axis in the $\sqrt{s}$ plane due to the absence of a real component. The roots of (9) are given below

$$\sqrt{s} = \frac{j}{2\sqrt{\tau}} \left[2\pi r_1 - 2\,tau^{-1}\Theta_1 \right] \qquad (18)$$
$$r_1 = 0, 1, 2, \ldots$$

Considering the second product term of (8) and solving for the root locations results in:

$$log_e \left(\frac{j\Theta_1 - 1}{j\Theta_1 + 1} \right) = log_e \left| \frac{j\Theta_1 - 1}{j\Theta_1 + 1} \right| + j\,2m\pi + j\,tau^{-1}\frac{2\Theta_1}{\Theta_1^2 - 1} \qquad (19)$$

again as before $\left| \dfrac{j\Theta_1 - 1}{j\Theta_1 + 1} \right| = 1$, resulting in the following roots

$$\sqrt{S} = \frac{j}{2\sqrt{\tau}} \left[\pi r_2 - 2 \tan^{-1} Q_1 \right] \qquad \begin{array}{l} r_2 = 2(m-n) + 1 \\ r_2 = 1, 2, \ldots \end{array} \qquad (20)$$

Note that equations (17) and (20) are identical.

Now, considering the roots of equation (6), namely

$$\tanh^2 \sqrt{\tau s} - \Theta_2^2 = 0 \qquad (21)$$

which can be represented by a product of two terms,

$$\left(\tanh \sqrt{\tau s} - \Theta_2 \right)\left(\tanh \sqrt{\tau s} + \Theta_2 \right) = 0 \qquad (22)$$

We consider the first term and use the same identity as in (10), therefore

$$\sinh \sqrt{\tau s} = \Theta_2 \cosh \sqrt{\tau s} \qquad (23)$$

or

$$e^{\sqrt{\tau s}} - e^{-\sqrt{\tau s}} = \Theta_2 \left[e^{\sqrt{\tau s}} + e^{-\sqrt{\tau s}} \right] \qquad (24)$$

Regrouping terms and dividing by $(\Theta_2 + 1) e^{-\sqrt{\tau s}}$ yields,

$$1 = \frac{\Theta_2 - 1}{\Theta_2 + 1} e^{2\sqrt{\tau s}} \qquad (25)$$

but

$$\left(\frac{\Theta_2 - 1}{\Theta_2 + 1} \right) = e^{\log_e \left(\frac{\Theta_2 - 1}{\Theta_2 + 1} \right)} \qquad (26)$$

where

$$\log_e \left(\frac{Q_2 - 1}{Q_2 + 1}\right) = \log_e \left|\frac{Q_2 - 1}{Q_2 + 1}\right| + j\, 2m\pi + j\, \Phi \qquad (27)$$

and $\Phi = 0, \pi \qquad$ for $\left(\frac{Q_2 - 1}{Q_2 + 1}\right) \begin{array}{c} \geq 0 \\ < 0 \end{array}$

Inserting (27) back into (25) yields

$$-1 = \left[e^{\log_e \left|\frac{Q_2 - 1}{Q_2 + 1}\right| + j\, 2m\pi + j\, \Phi}\right] e^{z\sqrt{\tau s}} \qquad (28)$$

but $\quad -1 = e^{j\pi + j\, 2n\pi} \qquad$ therefore (28) becomes

$$e^{j\pi + j\, 2n\pi} = \left[e^{\log_e \left|\frac{Q_2 - 1}{Q_2 + 1}\right| + j(2m\pi + \Phi)}\right] e^{z\sqrt{\tau s}} \qquad (29)$$

Solving for the roots of the first term of (22) yields

$$\sqrt{s} = \frac{1}{2\sqrt{\tau}} \log_e \left|\frac{Q_2 - 1}{Q_2 + 1}\right| + j\frac{1}{2\sqrt{\tau}} \left[\pi(r_3 + 1) - \Phi\right] \qquad (30)$$

$$r_3 = 2(n - m)$$
$$= 0, 1, 2, \cdots$$

A similar counterpart for equation (27) is obtained by solving for the roots of the second term of (22), namely

$$\log_e \left(\frac{1 + Q_2}{1 - Q_2}\right) = \log_e \left|\frac{1 + Q_2}{1 - Q_2}\right| + j\, 2m\pi + j\, \Phi \qquad (31)$$

$$\Phi = K\pi \quad K = 0, 1, 2, \ldots$$

and proceeding in a similar fashion as above, the second set of roots for (6) are given below by

$$\sqrt{s} = -\frac{1}{2\sqrt{\tau}} \log_e \left|\frac{1 + Q_2}{1 - Q_2}\right| - j\frac{1}{2\sqrt{\tau}} \left[\pi r_4 + \Phi\right] \qquad (32)$$

$$r_4 = 0, 1, 2, \ldots$$

BIBLIOGRAPHY

1. J.G. Linvill, "RC Active Filters," Proc. IRE,
    vol. 42, pp. 555-564, March, 1954.

2. T. Yanagisawa, "RC Active Networks Using Current
    Inversion Type Negative Impedance Converters,"
    IRE Trans. on Circuit Theory, vol. CT-4, pp. 140-144,
    September 1957.

3. J.M. Sipress, "Synthesis of Active RC Networks,"
    IRE Trans. on Circuit Theory, vol CT-9, pp.206-269,
    September, 1961.

4. I.W. Sandberg, "Active RC Networks," Research Report
    R662-58, PIB-590, Polytechnic Inst. of Brooklyn,
    N.Y., May, 1958.

5. B.K. Kinarawala, "Synthesis of Active RC Networks,"
    Bell System Tech. Journal, vol. 38,pp. 1269-1317,
    September 1959.

6. I.M. Horowitz, "Active RC Transfer Function Synthesis
    by Means of Cascaded RC and RL Structures,"
    Microwave Res. Inst., Polytechnic Inst. of Brooklyn,
    N.Y., Report No. R-507-56, pp. 113-437, 1956.

7. A.I. Larky, "Negative Impedance Converters,"
    IRE Trans. Circuit Theory, vol. 4, pp. 124-131,
    September, 1957.

8. R.W. Wyndrum Jr., "The Exact Synthesis of Distributed
    RC Networks," Tech. Report 400-76, Dept. Electrical
    Engineering, New York Univ., May, 1963.

9. R.P. O'Shea, "Synthesis Using Distributed RC
    Networks," IEEE Internat. Convention Record,
    part 7, pp. 18-29 , 1965.

10. E.A. Guillemin, "Synthesis of Passive Networks,"
    John Wiley and Sons, Inc., New York, 1957.

11. N. Balabanian, "Network Synthesis," Prentice Hall,
    Inc., 1958.

12. P.M. Chirlian, "Integrated and Active Network
    Analysis and Synthesis," Prentice Hall, Inc., 1967.

13. D.A. Calahan, "Modern Network Synthesis," Hayden
    Book Co., Inc., New York, 1964.

14. P.I. Richards, "Resistor Transmission Line Circuits,"
    Proc.IRE, vol. 30 No. 2, pp. 217-220, February, 1948.

15. J.O. Scanlan and J.D.Rhodes, "Realizability and
    Synthesis of a Restricted Class of Distributed RC
    Networks," IEEE Trans. Circuit Theory, vol. 12,
    pp. 577-585, December, 1965.

16. J. Stein, S. Shamis, and J. Mulligan, "Realization
    of Transfer Functions Using Uniform RC Distributed
    Networks with Common Ground Connections," Tech.
    Report 400-140, Dept. of Electrical Engineering,
    New York University, June 1966.